AD-A108 395 SYRACUSE UNIV NY DEPT OF ELECTRICAL AND COMPUTER EN--ETC F/G 20/3
ELECTROMAGNETIC COUPLING TO A CONDUCTING BODY OF REVOLUTION WIT--ETC(U)
JUL 81 J R MAUTZ, R F HARRINGTON F30602-79-C-0011

UNCLASSIFIED RADC-TR-81-202 NL

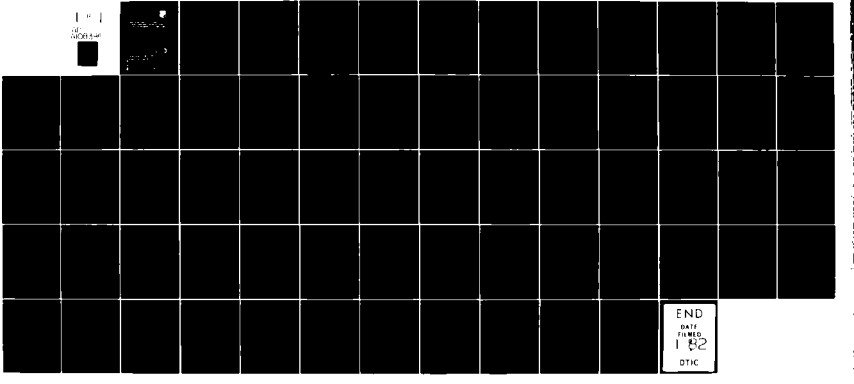

END
DATE FILMED
1 82
DTIC

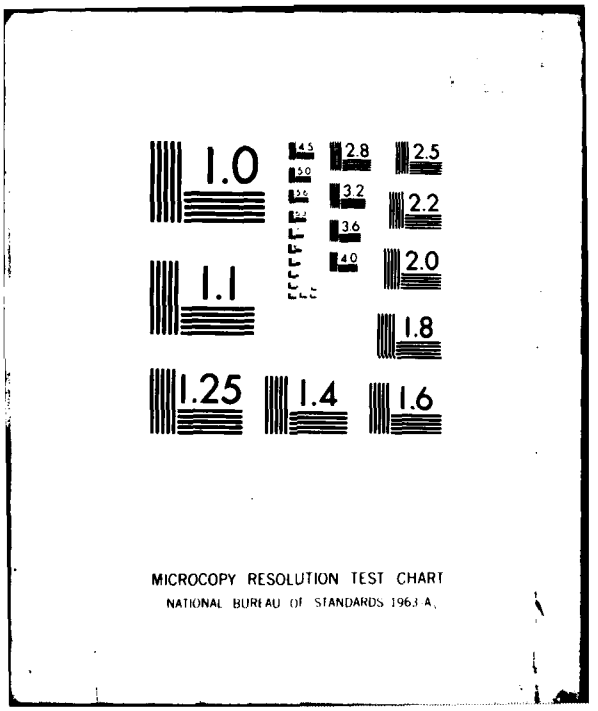
1.0
1.1
1.25
1.4
1.6
1.8
2.0
2.2
2.5
2.8
3.2
3.6
4.0
4.5
5.0
MICROCOPY RESOLUTION TEST CHART
NATIONAL BUREAU OF STANDARDS 1963 A.

RADC-TR-81-202
Final Report
July 1981

ELECTROMAGNETIC COUPLING TO A CONDUCTING BODY OF REVOLUTION WITH A HOMOGENEOUS MATERIAL REGION

Syracuse University

Joseph R. Mautz
Roger F. Harrington

ROME AIR DEVELOPMENT CENTER
Air Force Systems Command
Griffiss Air Force Base, New York 13441

UNCLASSIFIED

SECURITY CLASSIFICATION OF THIS PAGE (When Data Entered)

REPORT DOCUMENTATION PAGE		READ INSTRUCTIONS BEFORE COMPLETING FORM
1. REPORT NUMBER RADC-TR-81-202	2. GOVT ACCESSION NO. AD-A108 395	3. RECIPIENT'S CATALOG NUMBER
4. TITLE (and Subtitle) ELECTROMAGNETIC COUPLING TO A CONDUCTING BODY OF REVOLUTION WITH A HOMOGENEOUS MATERIAL REGION		5. TYPE OF REPORT & PERIOD COVERED Phase Report 6. PERFORMING ORG. REPORT NUMBER N/A
7. AUTHOR(s) Joseph R. Mautz Roger F. Harrington		8. CONTRACT OR GRANT NUMBER(s) F30602-79-C-0011
9. PERFORMING ORGANIZATION NAME AND ADDRESS Syracuse University Department of Electrical & Computer Engineering Syracuse NY 13210		10. PROGRAM ELEMENT, PROJECT, TASK AREA & WORK UNIT NUMBERS 62702F 23380317
11. CONTROLLING OFFICE NAME AND ADDRESS Rome Air Development Center (RBCT) Griffiss AFB NY 13441		12. REPORT DATE July 1981 13. NUMBER OF PAGES 66
14. MONITORING AGENCY NAME & ADDRESS(if different from Controlling Office) Same		15. SECURITY CLASS. (of this report) UNCLASSIFIED 15a. DECLASSIFICATION/DOWNGRADING SCHEDULE N/A

16. DISTRIBUTION STATEMENT (of this Report)

Approved for public release; distribution unlimited.

17. DISTRIBUTION STATEMENT (of the abstract entered in Block 20, if different from Report)

Same

18. SUPPLEMENTARY NOTES

RADC Project Engineer: Roy F. Stratton (RBCT)

19. KEY WORDS (Continue on reverse side if necessary and identify by block number)

Aperture coupling	Electromagnetic coupling
Body of Revolution	Homogeneous material region
Conductor plus dielectric	Method of moments

20. ABSTRACT (Continue on reverse side if necessary and identify by block number)

A numerical solution for electromagnetic coupling to a perfectly conducting body of revolution with a loss-free homogeneous material region is developed, ~~herein~~. The material region is exposed by a rotationally symmetric aperture in the conducting body. Application of the equivalence principle introduces an unknown electric current on the surface of the conducting body, and both an unknown equivalent electric current and an uninown equivalent magnetic current in the aperture. These currents satisfy the (Cont'd)

DD FORM 1 JAN 73 1473 EDITION OF 1 NOV 65 IS OBSOLETE

UNCLASSIFIED

SECURITY CLASSIFICATION OF THIS PAGE (When Data Entered)

4/6/81

Item 20 (Cont'd)

integral equations obtained by annihilating the tangential components of the electric field on the surface of the conducting body and by enforcing continuity of the tangential components of the electric and magnetic fields across the aperture. These integral equations are solved numerically by means of the method of moments.

Numerical results for the above mentioned currents are presented for four different conducting bodies, each of which has a dielectric region and is excited by an axially incident plane wave. The computer program that was used to calculate these currents allows for the more general case of oblique incidence. This program ~~will be~~ is described and listed along with sample input and output in a forthcoming report.

CONTENTS

		Page
I.	INTRODUCTION	1
II.	FORMULATION OF THE PROBLEM	1
III.	METHOD OF MOMENTS SOLUTION	7
IV.	ELIMINATION OF T_n FOR NEGATIVE VALUES OF n	21
V.	PLANE WAVE INCIDENCE	37
VI.	NUMERICAL RESULTS	42
REFERENCES		59

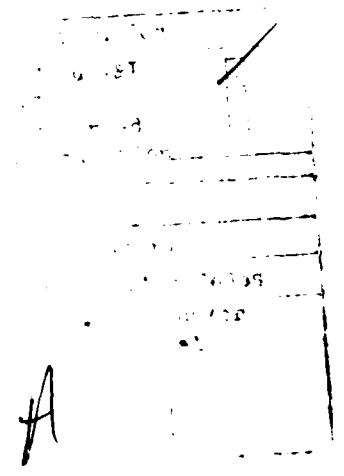

I. INTRODUCTION

A numerical solution to the problem of electromagnetic coupling to a perfectly conducting body of revolution with an interior region filled with a loss-free homogeneous material is developed here. Similar, but nevertheless different, problems have have already been solved. For example, numerical solutions for homogeneous material bodies of revolution appear in [1] and [2]. The problem of the lossy dielectric body of revolution is addressed in [3]. Multilayered bodies are considered in [4] and [5]. The problem of electromagnetic penetration through a sleeve-fit seam in an otherwise perfectly conducting surface of revolution is treated in [6]. Although the seam in [6] may exhibit a dielectric contrast, the bulk of the material inside the surface is the same as the material outside. The concept of equivalent currents [7, Sec. 3-5] is used in [1]-[5]. An equivalent aperture excitation technique [8] and an aperture loading technique are used in [6]. Inspiration for the aperture loading technique was drawn from [9].

Coupling to a perfectly conducting body of revolution with a homogeneous interior region is considered in [10], but no numerical solution is pursued there. In the present report, the boundary formulation consisting of [10, Eqs. (15)-(18)] is solved numerically by means of the method of moments [11]. This formulation is only one of several boundary formulations suggested in [10, Section 2]. More boundary formulations are outlined in [10, Sections, 3, 4, and 5]. Those in [10, Sections 4 and 5] take advantage of the technique of subtracting out the short-circuit fields. This technique captures the essence of the equivalent aperture excitation technique. The present report is exclusively devoted to the numerical solution of the particular boundary formulation consisting of [10, Eqs. (15)-(18)].

II. FORMULATION OF THE PROBLEM

The problem is that of electromagnetic coupling to the perfectly conducting body of revolution with homogeneous interior region shown in Fig. 1. Figure 1 shows a cross section of the configuration in a plane containing the axis (z axis) of the conducting body of revolution. This

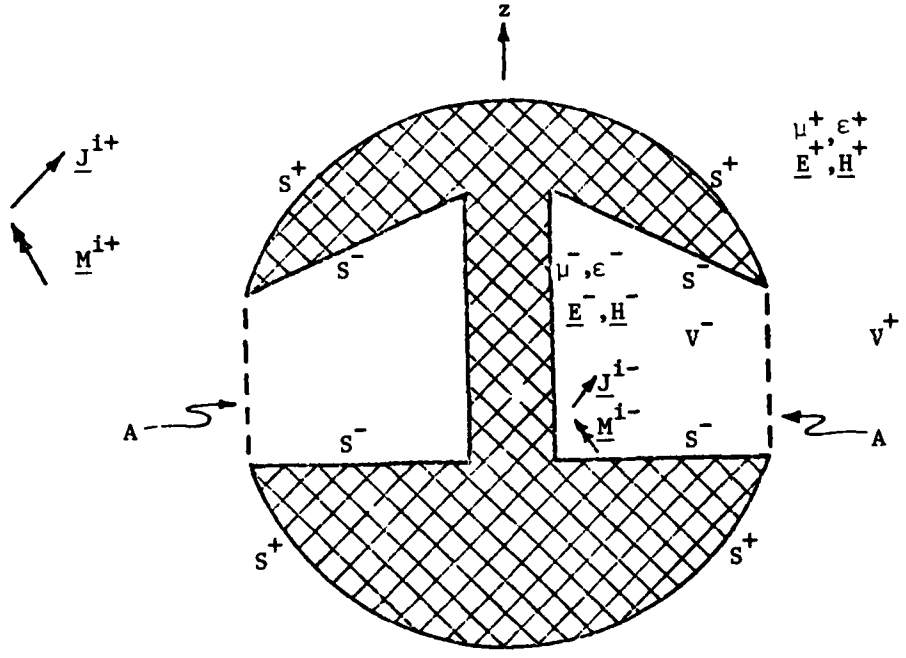

Fig. 1. Original problem.

conducting body is crosshatched. Homogeneous material with permeability μ^+ and permittivity ϵ^+ fills the exterior region V^+ bounded by the surface S^+ and the aperture A. What is called S^+ is not a single surface, but two surfaces, one below A and one above A. The interior region V^- bounded by the surface S^- and the aperture A is filled with homogeneous material characterized by μ^- and ϵ^-. All three surfaces S^+, S^-, and A are surfaces of revolution. The electromagnetic excitation consists of impressed electric and magnetic current sources $\underline{J}^{i+}$ and $\underline{M}^{i+}$ in V^+ and sources $\underline{J}^{i-}$ and $\underline{M}^{i-}$ in V^-. The resulting electric and magnetic fields in V^+ are called $\underline{E}^+$ and $\underline{H}^+$. The fields in V^- are called $\underline{E}^-$ and $\underline{H}^-$. The fields $\underline{E}^{\pm}$ and $\underline{H}^{\pm}$ are unknown. Obviously, solution for them constitutes a complete solution to the problem presented in Fig. 1. However, our solution will be for equivalent surface currents on $S^{\pm}$ and A rather than for the fields $\underline{E}^{\pm}$ and $\underline{H}^{\pm}$. It is possible to construct $\underline{E}^{\pm}$ and $\underline{H}^{\pm}$ from these equivalent surface currents, but this is not done in the present report.

The equivalence principle [7, Sec. 3-5] is used to obtain the situations shown in Figs. 2 and 3. In Fig. 2, ($\underline{J}^{i+}$, $\underline{M}^{i+}$) and equivalent currents $\underline{J}^+$, $\underline{J}$, and $\underline{M}$ radiate in the presence of the homogeneous medium (μ^+, ϵ^+) to produce ($\underline{E}^+$, $\underline{H}^+$) in V^+ and zero field elsewhere. Here, $\underline{J}^+$ is an electric current on S^+, $\underline{J}$ is an electric current on A, and $\underline{M}$ is a magnetic current on A. In Fig. 3, ($\underline{J}^{i-}$, $\underline{M}^{i-}$) and equivalent currents $-\underline{J}^-$, $-\underline{J}$, and $-\underline{M}$ radiate in the presence of the homogeneous medium (μ^-, ϵ^-) to produce ($\underline{E}^-$, $\underline{H}^-$) in V^- and zero field elsewhere. Here, $-\underline{J}^-$ is an electric current on S^-, $-\underline{J}$ is an electric current on A, and $-\underline{M}$ is a magnetic current on A. Since the surfaces S^+ and S^- are perfectly conducting in the original problem of Fig. 1, only equivalent electric currents are needed on them in Figs. 2 and 3. The choice of $-\underline{J}^-$ rather than $\underline{J}^-$ on S^- in Fig. 3 is due to personal preference. However, the minus sign relationship between the aperture currents in Figs. 2 and 3 is mandated by the zero field stipulations in Figs. 2 and 3 and continuity of the tangential components of the electric and magnetic fields across the aperture in Fig. 1. If the zero field stipulations in Figs. 2 and 3 are enforced, then the minus sign relationship between the aperture currents in Figs. 2 and 3 ensures continuity of tangential fields across the aperture in Fig. 1. However, if these zero field stipulations are not enforced, then the minus sign

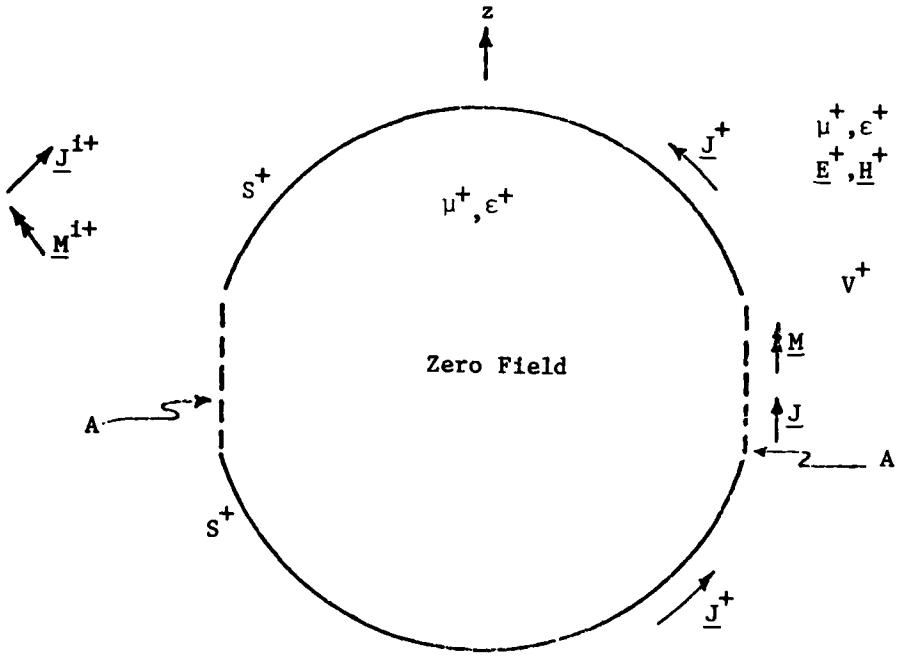

Fig. 2. Equivalence for region V^+.

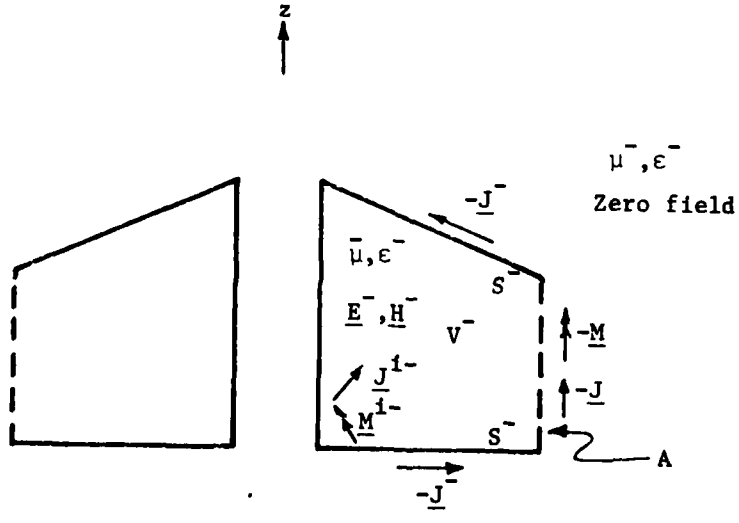

Fig. 3. Equivalence for region V^-.

relationship between the aperture currents does not ensure continuity of the tangential fields across the aperture in Fig. 1.

The equivalence principle states that the equivalent currents in Figs. 2 and 3 are unique, but does not tell how to determine them. The expressions in [7, Sec. 3-5] for the equivalent currents in terms of the tangential components of the fields can not be used because the fields are not known either. We determine the equivalent currents by enforcing the boundary conditions for the fields in Fig. 1. These boundary conditions are:

1) The tangential components of the electric field vanish on the conducting surface S^+.

2) The tangential components of the electric field vanish on the conducting surface S^-.

3) The tangential components of the electric field are continuous across the aperture A.

4) The tangential components of the magnetic field are continuous across the aperture A.

The equations for these four boundary conditions are

$$\frac{1}{\eta^+} \underline{E}^+_{tan} = 0 \qquad \text{on } S^+ \tag{1a}$$

$$\frac{1}{\eta^+} \underline{E}^-_{tan} = 0 \qquad \text{on } S^- \tag{1b}$$

$$\frac{1}{\eta^+} \underline{E}^+_{tan} = \frac{1}{\eta^+} \underline{E}^-_{tan} \qquad \text{on A} \tag{1c}$$

$$\underline{H}^+_{tan} = \underline{H}^-_{tan} \qquad \text{on A} \tag{1d}$$

The subscript "tan" denotes tangential components on the surface in question. The factor

$$\frac{1}{\eta^+} = \sqrt{\frac{\varepsilon^+}{\mu^+}} \tag{2}$$

was included in (1) to make (1a), (1b), and (1c) compatible with (1d).

In view of Figs. 2 and 3, (1) can be rewritten as

$$-\frac{1}{\eta^+}\underline{E}^+_{tan}(\underline{J}^+ + \underline{J}, \underline{M}) = \frac{1}{\eta^+}\underline{E}^{i+}_{tan} \qquad \text{on } S^+ \tag{3a}$$

$$-\frac{1}{\eta^+}\underline{E}^-_{tan}(\underline{J}^- + \underline{J}, \underline{M}) = -\frac{1}{\eta^+}\underline{E}^{i-}_{tan} \qquad \text{on } S^- \tag{3b}$$

$$-\frac{1}{\eta^+}\underline{E}^+_{tan}(\underline{J}^+ + \underline{J}, \underline{M}) - \frac{1}{\eta^+}\underline{E}^-_{tan}(\underline{J}^- + \underline{J}, \underline{M}) = \frac{1}{\eta^+}\underline{E}^{i+}_{tan} - \frac{1}{\eta^+}\underline{E}^{i-}_{tan} \qquad \text{on A} \tag{3c}$$

$$-\underline{H}^+_{tan}(\underline{J}^+ + \underline{J}, \underline{M}) - \underline{H}^-_{tan}(\underline{J}^- + \underline{J}, \underline{M}) = \underline{H}^{i+}_{tan} - \underline{H}^{i-}_{tan} \qquad \text{on A} \tag{3d}$$

where $\underline{E}^{\pm}_{tan}(\underline{J}, \underline{M})$ denotes the tangential components of the electric field due to the electric current $\underline{J}$ and the magnetic current $\underline{M}$, both radiating in the medium characterized by $(\mu^{\pm}, \varepsilon^{\pm})$. Similarly, $\underline{H}^{\pm}_{tan}(\underline{J}, \underline{M})$ denotes the tangential components of the corresponding magnetic field. $\underline{E}^{i\pm}_{tan}$ and $\underline{H}^{i\pm}_{tan}$ are the tangential electric and magnetic fields due to $(\underline{J}^{i\pm}, \underline{M}^{i\pm})$ radiating in the medium characterized by $(\mu^{\pm}, \varepsilon^{\pm})$. Since $\underline{J}^+$ and $\underline{J}$ are disjoint, the + sign between them in the expression $(\underline{J}^+ + \underline{J})$ means union rather than simple addition. Similarly, $(\underline{J}^- + \underline{J})$ denotes the union of $\underline{J}^-$ with $\underline{J}$. It does not matter whether the tangential electric fields on the left-hand sides of (3a) and (3b) are evaluated just inside $S^{\pm}$ or just outside $S^{\pm}$ because they are continuous across $S^{\pm}$. The Ampere's law contributions cancel out of the left-hand sides of (3c) and (3d). By Ampere's law contribution we mean the contribution to the field due to the value of the current at the field point. The qualification "on A" in (3c) and (3d) means not only evaluation on A but also suppression of all Ampere's law contributions. The set of equations (3) is essentially the same as [10, Eqs. (15)-(18)]. It is shown in [10] that these equations suffice to uniquely determine the equivalent currents $\underline{J}^{\pm}$, $\underline{J}$, and $\underline{M}$.

The four field operators which give the electric and magnetic fields due to electric and magnetic currents appear in (3). However, it is evident from [7, Eq. 3-79)] that

$$\underline{E}^{\pm}_{tan}(0, \underline{M}) = -\eta^+ \underline{H}^{\pm}_{tan}(\frac{1}{\eta^+}\underline{M}, 0) \tag{4}$$

$$\underline{H}^{\mp}_{tan}(0, \underline{M}) = \frac{\eta^+}{(\eta^{\pm})^2}\underline{E}^{\pm}_{tan}(\frac{1}{\eta^+}\underline{M}, 0) \tag{5}$$

where

$$\eta^{+} = \sqrt{\frac{\mu^{+}}{\epsilon^{+}}} \tag{6}$$

The seemingly superfluous pair of factors η^{+} and $1/\eta^{+}$ on the right-hand sides of (4) and (5) were included in order to liken the first arguments of $\underline{E}^{i}_{tan}$ and $\underline{H}^{i}_{tan}$ to electric currents. In view of linearity of the field operators, substitution of (4) and (5) into (3) gives

$$-\frac{1}{\eta^{+}}\underline{E}^{+}_{tan}(\underline{J}^{+}+\underline{J},0) + \underline{H}^{+}_{tan}\left(\frac{1}{\eta^{+}}\underline{M},\ 0\right) = \frac{1}{\eta^{+}}\underline{E}^{i+}_{tan} \qquad \text{on } S^{+} \tag{7a}$$

$$-\frac{1}{\eta^{+}}\underline{E}^{-}_{tan}(\underline{J}^{-}+\underline{J},0) + \underline{H}^{-}_{tan}\left(\frac{1}{\eta^{+}}\underline{M},0\right) = -\frac{1}{\eta^{+}}\underline{E}^{i-}_{tan} \qquad \text{on } S^{-} \tag{7b}$$

$$-\frac{1}{\eta^{+}}\underline{E}^{+}_{tan}(\underline{J}^{+}+\underline{J},0) - \frac{1}{\eta^{+}}\underline{E}^{-}_{tan}(\underline{J}^{-}+\underline{J},0) + \underline{H}^{+}_{tan}\left(\frac{1}{\eta^{+}}\underline{M},0\right) + \underline{H}^{-}_{tan}\left(\frac{1}{\eta^{+}}\underline{M},0\right)$$

$$= \frac{1}{\eta^{+}}\underline{E}^{i+}_{tan} - \frac{1}{\eta^{+}}\underline{E}^{i-}_{tan} \qquad \text{on A} \tag{7c}$$

$$-\underline{H}^{+}_{tan}(\underline{J}^{+}+\underline{J},0) - \underline{H}^{-}_{tan}(\underline{J}^{-}+\underline{J},0) - \frac{1}{\eta^{+}}\underline{E}^{+}_{tan}\left(\frac{1}{\eta^{+}}\underline{M},0\right) - \frac{\eta^{+}}{(\eta^{-})^{2}}\underline{E}^{-}_{tan}\left(\frac{1}{\eta^{+}}\underline{M},0\right)$$

$$= \underline{H}^{i+}_{tan} - \underline{H}^{i-}_{tan} \qquad \text{on A} \tag{7d}$$

Unlike the left-hand sides of (3) which contain all four field operators, the left-hand sides of (7) contain only the operators which give the electric and magnetic fields due to electric currents. Equations (7) are solved by means of the method of moments in section III.

III. METHOD OF MOMENTS SOLUTION

The method of moments solution to (7) is obtained by first expressing the unknown currents $(\underline{J}^{+}+\underline{J})$, $(\underline{J}^{-}+\underline{J})$, and $\underline{M}$ as linear combinations of known expansion functions, then taking the symmetric product of (7) with each member of a set of testing functions, and finally solving the resulting set of simultaneous equations.

Momentarily ignoring the fact that $(\underline{J}^{+}+\underline{J})$ and $(\underline{J}^{-}+\underline{J})$ are supposed to be equal on A, we write

$$\underline{J}^{+}+\underline{J} = \sum_{n}\left[\sum_{j=1}^{N^{+}-2} I_{nj}^{t+}\,\underline{J}_{nj}^{t+} + \sum_{j=1}^{N^{+}-1} I_{nj}^{\phi+}\,\underline{J}_{nj}^{\phi+}\right] \quad \text{on } (S^{+}+A) \tag{8}$$

$$\underline{J}^{-}+\underline{J} = \sum_{n}\left[\sum_{j=1}^{N^{-}-2} I_{nj}^{t-}\,\underline{J}_{nj}^{t-} + \sum_{j=1}^{N^{-}-2} I_{nj}^{\phi-}\,\underline{J}_{nj}^{\phi-}\right] \quad \text{on } (S^{-}+A) \tag{9}$$

where $(S^{+}+A)$ is the surface which is the union of S^{+} and A. Similarly, $(S^{-}+A)$ is the union of S^{-} and A. Since S^{+}, S^{-}, and A are surfaces of revolution, $(S^{+}+A)$ and $(S^{-}+A)$ are also surfaces of revolution. In (8) and (9), I_{nj}^{t+} and $I_{nj}^{\phi+}$ are unknown coefficients. The vectors $\underline{J}_{nj}^{t\pm}$ and $\underline{J}_{nj}^{\phi\pm}$ in (8) and (9) are expansion functions defined by

$$\underline{J}_{nj}^{t\pm} = \underline{u}_{t\pm}\,\frac{T_{j}^{\pm}(t^{\pm})}{\rho^{\pm}}\,e^{jn\phi} \qquad \begin{cases} j = 1,2,\ldots N^{\pm}-2 \\ n = 0, \pm1, \pm2,\ldots \end{cases} \tag{10a}$$

$$\underline{J}_{nj}^{\phi\pm} = \underline{u}_{\phi}\,\frac{P_{j}^{\pm}(t^{\pm})}{\rho_{j}^{\pm}}\,e^{jn\phi} \qquad \begin{cases} j = 1,2,\ldots (N^{+}-1 \text{ or } N^{-}-2) \\ n = 0, \pm1, \pm2,\ldots \end{cases} \tag{10b}$$

The right-hand sides of (10) were obtained by attaching the superscript $\pm$ to various quantities in the version of [12, Eqs. (2) and (3)] with P replaced by N. The notation $\pm$ in (10) denotes quantities defined on $(S^{\pm}+A)$. The subscript j which runs from 1 to either $N^{\pm}-2$, $N^{+}-1$, or $N^{-}-2$ in (10) is not to be confused with the j which appears in the argument of the exponential in (10). The latter j is $\sqrt{-1}$.

The quantities decorated with the notation $\pm$ on the right-hand side of (10) depend on the generating curve of the surface $(S^{\pm}+A)$. The generating curve of a surface of revolution is the plane curve, which when rotated about the z axis, generates the surface of revolution. For computations, the generating curve of $(S^{\pm}+A)$ is approximated by choosing a succession of points $\bar{t}_{j}^{\pm}$, $j=1,2,\ldots N^{\pm}$, on the generating curve of $(S^{\pm}+A)$ and then connecting them with straight line segments. The point $\bar{t}_{j}^{\pm}$ is called a data point. Its location is specified by its distance $\bar{\rho}_{j}^{\pm}$ from the z axis and its z coordinate $\bar{z}_{j}^{\pm}$. Hence, we write

$$\text{Location of } \bar{t}_j^{\pm} = (\bar{\rho}_j^{\pm}, \bar{z}_j^{\pm}), \quad j = 1,2,\ldots N^{\pm} \tag{11}$$

The generating curve of $(S^{+}+A)$ starts at $\bar{t}_1^{\pm}$, goes to $\bar{t}_2^{+}$, then to $\bar{t}_3^{\pm}$, and so forth until the last data point $\bar{t}_{N^{\pm}}^{\pm}$ is reached. A typical arrangement of data points on the generating curve of $(S^{+}+A)$ is shown in Fig. 4. Figure 5 shows an arrangement of data points on the generating curve of $(S^{-}+A)$. The first and last data points on the generating curve of $(S^{+}+A)$ are on the z axis. The last two data points on the generating curve of $(S^{-}+A)$ overlap with the first two. All data points on A are common to the generating curves of both $(S^{+}+A)$ and $(S^{-}+A)$. There are M data points on A. The first data point on A is the point where A meets the lower part of S^{+}. This data point is the $(M^{\pm}+1)$th data point on the generating curve of $(S^{\pm}+A)$. The last data point on A is the point where A meets the upper part of S^{+}.

In (10), ϕ is the angular distance from the positive x axis. ϕ is measured in the xy plane and toward the positive y axis. In (10b), $\underline{u}_{\phi}$ is the unit vector in the ϕ direction. No $\pm$ needs to be attached to ϕ and $\underline{u}_{\phi}$ because they do not depend on the generating curve of $(S^{\pm}+A)$.

Henceforth, the expression "generating curve of $(S^{\pm}+A)$" will mean the series of straight line segments connecting the data points $\bar{t}_j^{\pm}$, $j=1,2,\ldots N^{\pm}$. In (10), $t^{\pm}$ is the arc length along the generating curve of $(S^{\pm}+A)$ and $\underline{u}_{t^{\pm}}$ is the unit vector in the $t^{\pm}$ direction. We choose $t^{\pm}$ to be zero at the data point $\bar{t}_1^{\pm}$ where the generating curve of $(S^{\pm}+A)$ starts. Previously, only the location of $\bar{t}_j^{\pm}$ was specified. The value of $\bar{t}_j^{\pm}$ is now defined to be the value of $t^{\pm}$ at the location of $\bar{t}_j^{\pm}$. In (10a), $T_j^{\pm}(t^{\pm})$ is the triangle function which starts at $t^{\pm} = \bar{t}_j^{\pm}$, reaches the maximum height of unity at $t^{\pm} = \bar{t}_{j+1}^{\pm}$, and ends at $t^{\pm} = \bar{t}_{j+2}^{\pm}$. In (10b), $P_j^{\pm}(t^{\pm})$ is the unit pulse function which starts at $t^{\pm} = \bar{t}_j^{\pm}$ and ends at $t^{\pm} = \bar{t}_{j+1}^{\pm}$. Naturally, the functions $T_j^{\pm}$ and $P_j^{\pm}$ are real. They are essentially the same as the functions T_j and P_j shown in [12, Figs. 1 and 2]. The $\bar{t}_j$ used in [12] corresponds to $\bar{t}_j^{-}$ of the present report. The notation of the present report was obtained by replacing the superscript - on t_j in [12] by a horizontal bar directly above t_j and then appending the superscript $^{+}$. In (10a), $\rho^{\pm}$ is the distance from the z axis at $t^{\pm}$.

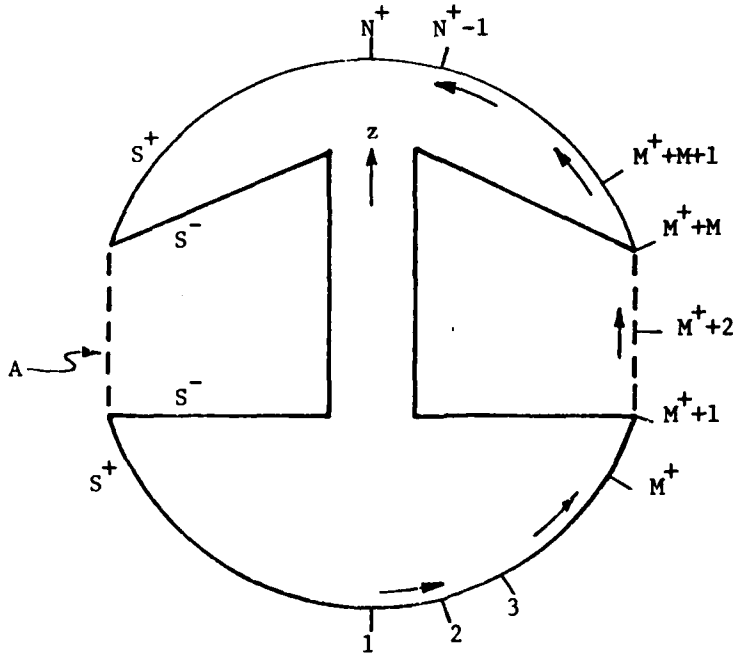

Fig. 4. Arrangement of data points on the generating curve of the surface ($S^+ + A$).

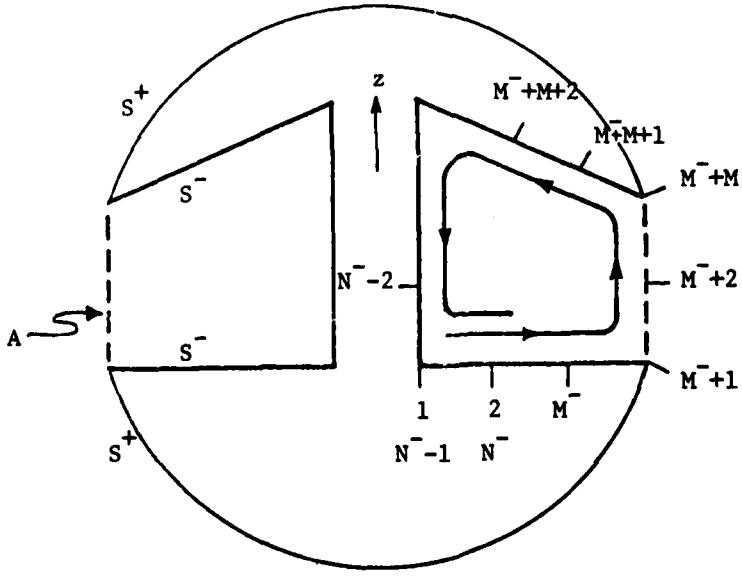

Fig. 5. Arrangement of data points on the generating curve of the surface ($S^- + A$).

In (10b), $\rho_j^{\pm}$ is the value of $\rho^{\pm}$ at the center of the pulse function $P_j^{\pm}$. Because of the nature of the approximate generating curve of $(S^{\pm}+A)$,

$$\rho_j^{\pm} = \frac{1}{2}\,(\bar{\rho}_j^{\pm} + \bar{\rho}_{j+1}^{\pm}) \tag{12}$$

where, as previously defined, $\bar{\rho}_j^{\pm}$ is the distance of the data point $\bar{t}_j^{\pm}$ from the z axis. With the advent of $t^{\pm}$ and $\rho^{\pm}$, $\bar{\rho}_j^{\pm}$ becomes the value of $\rho^{\pm}$ at $t^{\pm} = \bar{t}_j^{\pm}$.

As is evident from the range of values of j in (10a), a peak of a triangle function is placed at each data point on the generating curve of $(S^{+}+A)$ except the first data point $\bar{t}_1^{+}$ and the last data point $\bar{t}_{N^+}^{+}$. As shown in Fig. 4, the data points $\bar{t}_1^{+}$ and $\bar{t}_{N^+}^{+}$ lie on the z axis. No peak of a triangle function is needed at $\bar{t}_1^{+}$ because the function $T_1^{+}(t^{+})/\rho^{+}$ in (10a), being equal to $1/\bar{\rho}_2^{+}$ for $\bar{t}_1^{+} \le t^{+} \le \bar{t}_2^{+}$, is just as large at $\bar{t}_1^{+}$ as it is at $\bar{t}_2^{+}$. Similarly, no peak of a triangle function is needed at $\bar{t}_{N^+}^{+}$ because the function $T_{N^+-2}^{+}(t^{+})/\rho^{+}$ in (10a) holds its value $1/\bar{\rho}_{N^+-1}^{+}$ at $t^{+} = \bar{t}_{N^+-1}^{+}$ all the way out to $t^{+} = \bar{t}_{N^+}^{+}$.

It was necessary to overlap the last two data points with the first two in Fig. 5 in order to induce a computational procedure which places no peak of a triangle function at the first and last data points to obtain a peak of a triangle function at every data point on the generating curve of $(S^{-}+A)$. The above mentioned computational procedure was originally designed for a generating curve such as that of $(S^{+}+A)$ whose first and last data points are on the z axis where no peaks of triangle functions are wanted. The second summation with respect to j in (9) is terminated at $j = N^{-}-2$ rather than at $j = N^{-}-1$ because, due to the overlapping data points in Fig. 5, the vector function $\underline{J}_{\underline{n},N^-1}^{\phi-}$ defined by setting $j = N^{-}-1$ in (10b) is a duplicate of $\underline{J}_{\underline{n}1}^{\phi-}$.

Because each triangle function in (10a) is continuous in $t^{\pm}$, the $t^{\pm}$ components of (8) and (9) are also continuous in $t^{\pm}$. As a result, (8) and (9) do not give rise to any circular loops of filamentary electric charge. Any circular loop of such charge is not physically realizable because an infinite amount of energy is required to assemble it. Since each pulse function in (10b) begins and ends abruptly, discontinuities

in the ϕ components of (8) and (9) are allowed at all the data points. Unlike discontinuities in the $t^{\pm}$ component of electric current, discontinuities in the ϕ component of electric current are not accompanied by concentrations of electric change.

Since the data points of the generating curves of $(S^{+}+A)$ and $(S^{-}+A)$ coincide with each other on A, the vector functions $\underline{J}^{t+}_{nj}$ and $\underline{J}^{\phi+}_{nj}$ on A in (8) are the same as those on A in (9). Hence, (8) and (9) can be made equal on A by equating the coefficients of these vector functions. We write

$$\underline{J}^{+}+\underline{J} = \sum_{n}\left[\sum_{j=1}^{M^{+}-1} I^{t+}_{nj}\underline{J}^{t+}_{nj} + \sum_{j=1}^{M^{+}} I^{\phi+}_{nj}\underline{J}^{\phi+}_{nj} + \sum_{j=M^{+}+M}^{N^{+}-2} I^{t+}_{nj}\underline{J}^{t+}_{nj} + \sum_{j=M^{+}+M}^{N^{+}-1} I^{\phi+}_{nj}\underline{J}^{\phi+}_{nj}\right]$$
$$+ \sum_{n}\left[\sum_{j=1}^{M} I_{nj}\underline{J}^{t+}_{n,j+M^{+}-1} + \sum_{j=1}^{M-1} I_{n,j+M}\underline{J}^{\phi+}_{n,j+M^{+}}\right] \tag{13}$$

$$\underline{J}^{-}+\underline{J} = \sum_{n}\left[\sum_{j=1}^{M^{-}-1} I^{t-}_{nj}\underline{J}^{t-}_{nj} + \sum_{j=1}^{M^{-}} I^{\phi-}_{nj}\underline{J}^{\phi-}_{nj} + \sum_{j=M^{-}+M}^{N^{-}-2} I^{t-}_{nj}\underline{J}^{t-}_{nj} + \sum_{j=M^{-}+M}^{N^{-}-2} I^{\phi-}_{nj}\underline{J}^{\phi-}_{nj}\right]$$
$$+ \sum_{n}\left[\sum_{j=1}^{M} I_{nj}\underline{J}^{t-}_{n,j+M^{-}-1} + \sum_{j=1}^{M-1} I_{n,j+M}\underline{J}^{\phi-}_{n,j+M^{-}}\right] \tag{14}$$

with

$$\underline{J}^{t+}_{nM^{+}} = \underline{J}^{t-}_{nM^{-}} \quad \text{on A} \tag{15a}$$

$$\underline{J}^{t+}_{n,j+M^{+}-1} = \underline{J}^{t-}_{n,j+M^{-}-1}, \quad j = 2,3,\ldots M-1 \tag{15b}$$

$$\underline{J}^{t+}_{n,M+M^{+}-1} = \underline{J}^{t-}_{n,M+M^{-}-1} \quad \text{on A} \tag{15c}$$

$$\underline{J}^{\phi+}_{n,j+M^{+}} = \underline{J}^{\phi-}_{n,j+M^{-}}, \quad j = 1,2,\ldots M-1 \tag{15d}$$

The coefficients that were equated in (8) and (9) have been relabeled I_{nj} and $I_{n,j+M}$ in (13) and (14). The first $\sum_{n}$ in (13) is a vector function confined to S^{+}. The vector functions $\underline{J}^{t+}_{nM^{+}}$ and $\underline{J}^{t+}_{n,M+M^{+}-1}$ in (13) straddle S^{+} and A. Except for the overflow of $\underline{J}^{t+}_{nM^{+}}$ and $\underline{J}^{t+}_{n,M+M^{+}-1}$ onto

S^+, the second $\sum_n$ in (13) is a vector function confined to A. The first $\sum_n$ in (14) is confined to S^-. The vector functions $\underline{J}^{t-}_{nM^-}$ and $\underline{J}^{t-}_{n,M+M^--1}$ in (14) straddle S^- and A. Except for the overflow of $\underline{J}^{t-}_{nM^-}$ and $\underline{J}^{t-}_{n,M+M^--1}$ onto S^-, the second $\sum_n$ in (14) is confined to A. The right-hand sides of (13) and (14) are equal on A because (15) implies that the portion on A of the second $\sum_n$ in (13) is equal to the portion on A of the second $\sum_n$ in (14).

To condense the notation in (13) and (14), we define expansion functions $\underline{J}^{1\pm}_{nj}$ and $\underline{J}^{2\pm}_{nj}$ by

$$\underline{J}^{1+}_{nj} = \begin{cases} \underline{J}^{t\pm}_{nj} & , \ j = 1,2,\ldots M^{\pm}-1 \\ \underline{J}^{\phi\pm}_{n,j-M^{\pm}+1} & , \ j = M^{\pm}, M^{\pm}+1,\ldots 2M^{\pm}-1 \\ \underline{J}^{t\pm}_{n,j-M^{\pm}+M} & , \ j = 2M^{\pm}, 2M^{\pm}+1,\ldots N^{\pm}+M^{\pm}-M-2 \\ \underline{J}^{\phi\pm}_{n,j-N^{\pm}+2M+1}, & j = N^{\pm}+M^{\pm}-M-1\ldots \begin{cases} 2N^+-2M-2 \\ \text{or } 2N^--2M-3 \end{cases} \end{cases} \tag{16}$$

$$\underline{J}^{2\pm}_{nj} = \begin{cases} \underline{J}^{t\pm}_{n,j+M^{\pm}-1} & , \quad j = 1,2,\ldots M \\ \underline{J}^{\phi\pm}_{n,j+M^{\pm}-M} & , \quad j = M+1, M+2,\ldots 2M-1 \end{cases} \tag{17}$$

and coefficients $I^{1\pm}_{nj}$ by

$$I^{1\pm}_{nj} = \begin{cases} I^{t\pm}_{nj} & , \ j = 1,2,..M^{\pm}-1 \\ I^{\phi\pm}_{n,j-M^{\pm}+1} & , \ j = M^{\pm}, M^{\pm}+1, \ldots 2M^{\pm}-1 \\ I^{t\pm}_{n,j-M^{\pm}+M} & , \ j = 2M^{\pm}, 2M^{\pm}+1,\ldots N^{\pm}+M^{\pm}-M-2 \\ I^{\phi\pm}_{n,j-N^{\pm}+2M+1}, & j = N^{\pm}+M^{\pm}-M-1,\ldots \begin{cases} 2N^+-2M-2 \\ \text{or } 2N^--2M-3 \end{cases} \end{cases} \tag{18}$$

The new vector functions (16) and (17) and the new coefficients (18) reduce (13) and (14) to

$$\underline{J}^{+}+\underline{J} = \sum_{n}\left[\sum_{j=1}^{2N^{+}-2M-2} I_{nj}^{1+}\underline{J}_{nj}^{1+} + \sum_{j=1}^{2M-1} I_{nj}\underline{J}_{nj}^{2+}\right] \tag{19}$$

$$\underline{J}^{-}+\underline{J} = \sum_{n}\left[\sum_{j=1}^{2N^{-}-2M-3} I_{nj}^{1-}\underline{J}_{nj}^{1-} + \sum_{j=1}^{2M-1} I_{nj}\underline{J}_{nj}^{2-}\right] \tag{20}$$

The first $\sum_{j}$ in (19) is on S^{+}. The functions $\underline{J}_{n1}^{2+}$ and $\underline{J}_{n,2M-1}^{2+}$ in (19) straddle S^{+} and A. Except for the overflow of $\underline{J}_{n1}^{2+}$ and $\underline{J}_{n,2M-1}^{2+}$ onto S^{+}, the second $\sum_{j}$ in (19) is confined to A. The first $\sum_{j}$ in (20) is on S^{-}. The functions $\underline{J}_{n1}^{2-}$ and $\underline{J}_{n,2M-1}^{2-}$ in (20) straddle S^{-} and A. Except for the overflow of $\underline{J}_{n1}^{2-}$ and $\underline{J}_{n,2M-1}^{2-}$ onto S^{-}, the second $\sum_{j}$ in (20) is confined to A. The right-hand sides of (19) and (20) are equal to each other on A.

The equivalent magnetic current $\underline{M}$ *in (7) is expanded as*

$$\underline{M} = \eta^{+}\sum_{n}\sum_{j=1}^{2M-3} V_{nj}\underline{J}_{nj}^{3+} \tag{21}$$

where V_{nj} is an unknown coefficient and $\underline{J}_{nj}^{3+}$ is an expansion function given by

$$\underline{J}_{nj}^{3+} = \begin{cases} \underline{J}_{n,j+M^{+}}^{t+} & , \; j = 1,2,\ldots M-2 \\ \underline{J}_{n,j+M^{+}-M+2}^{\phi+} & , \; j = M-1,\; M,\ldots 2M-3 \end{cases} \tag{22}$$

The t^{+} component of (21) is continuous so that no circular loops of filamentary magnetic charge appear in the aperture in Figs. 2 and 3. The ϕ component of (21) can have a discontinuity at each data point in the aperture.

Now that the expansions (19)-(21) have been written for the equivalent currents, the next step in the method of moments is to take the symmetric product of (7) with each member of a set of testing functions. The symmetric product of two vectors $\underline{W}$ and $\underline{E}$ is called $\langle W,E\rangle$ and is

defined to be the integral of the dot product of $\underline{W}$ with $\underline{E}$ over S^+, S^-, and A. First, (7a) is tested with the vector function $\underline{W}_{ni}^{1+}$ defined by

$$\underline{W}_{ni}^{1+} = (\underline{J}_{ni}^{1+})^* , \qquad i = 1,2,\ldots 2N^+-2M-2 \tag{23}$$

where the asterisk denotes complex conjugate. Then, (7b) is tested with

$$\underline{W}_{ni}^{1-} = (\underline{J}_{ni}^{1-})^* , \qquad i = 1,2,\ldots 2N^--2M-3 \tag{24}$$

For the sake of argument, we write

$$-\frac{1}{\eta^+}\underline{E}_{tan}^{+}(\underline{J}^+ + \underline{J},0) + \underline{H}_{tan}^{+}(\frac{1}{\eta^+}\underline{M},0) = \frac{1}{\eta^+}\underline{E}_{tan}^{i+} \qquad \text{on } (S^+ + A) \tag{25}$$

$$-\frac{1}{\eta^+}\underline{E}_{tan}^{-}(\underline{J}^- + \underline{J},0) + \underline{H}_{tan}^{-}(\frac{1}{\eta^+}\underline{M},0) = -\frac{1}{\eta^+}\underline{E}_{tan}^{i-} \qquad \text{on } (S^- + A) \tag{26}$$

Testing functions $\underline{W}_{ni}^{2+}$ and $\underline{W}_{ni}^{2-}$ are defined by

$$\underline{W}_{ni}^{2+} = (\underline{J}_{ni}^{2+})^* , \qquad i = 1,2,\ldots 2M-1 \tag{27}$$

$$\underline{W}_{ni}^{2-} = (\underline{J}_{ni}^{2-})^* , \qquad i = 1,2,\ldots 2M-1 \tag{28}$$

For a particular value of i, (25) is tested with $\underline{W}_{ni}^{2+}$, (26) is tested with $\underline{W}_{ni}^{2-}$, and the results are added to obtain one equation. Letting i run from 1 to 2M-1, we obtain 2M-1 equations. This kind of testing is equivalent to

1) Testing (7a) with the part of $\underline{W}_{n1}^{2+}$ on S^+,
   testing (7b) with the part of $\underline{W}_{n1}^{2-}$ on S^-,
   testing (7c) with the part of $\underline{W}_{n1}^{2+}$ on A,
   and adding the results to obtain one equation.
2) Testing (7c) with $\underline{W}_{ni}^{2+}$ for i = 2,3,...M-1

3) Testing (7a) with the part of $\underline{W}_{nM}^{2+}$ on S^+,
testing (7b) with the part of $\underline{W}_{nM}^{2-}$ on S^-,
testing (7c) with the part of $\underline{W}_{nM}^{2+}$ on A,
and adding the results to obtain one more equation.

4) Testing (7c) with $\underline{W}_{ni}^{2+}$ for i = M+1, M+2,...2M-1.

Statement 1) is justified in the following manner. Testing (25) with the part of $\underline{W}_{n1}^{2+}$ on S^+ is equivalent to testing (7a) with the part of $\underline{W}_{n1}^{2+}$ on S^+ because (7a) and (25) are identical on S^+. Likewise, testing (26) with the part of $\underline{W}_{n1}^{2-}$ on S^- is equivalent to testing (7b) with the part of $\underline{W}_{n1}^{2-}$ on S^-. It is evident from (27), (28), (17), and (15) that

$$\underline{W}_{ni}^{2+} = \underline{W}_{ni}^{2-} \quad \text{on A}, \quad i = 1,2,...2M-1 \tag{29a}$$

Hence, testing (25) with the part of $\underline{W}_{n1}^{2+}$ on A, testing (26) with the part of $\underline{W}_{n1}^{2-}$ on A, and adding the results is equivalent to testing the sum of (25) and (26) with the part of $\underline{W}_{n1}^{2+}$ on A. Because the sum of (25) and (26) on A is precisely (7c), this amounts to testing (7c) with the part of $\underline{W}_{n1}^{2+}$ on A. Consequently, statement 1) is true.

Since all the testing functions in statements 2) and 4) are confined to A, (29a) implies that

$$\underline{W}_{ni}^{2+} = \underline{W}_{ni}^{2-} \tag{29b}$$

for all the values of i in statements 2) and 4). Hence, for these values of i, testing (25) with $\underline{W}_{ni}^{2+}$, testing (26) with $\underline{W}_{ni}^{2-}$, and adding the results amounts to testing (7c) with $\underline{W}_{ni}^{2+}$ because the sum of (25) and (26) on A is (7c). Thus, statements 2) and 4) are true. Justification for statement 3) is similar to that for statement 1) and is left as an exercise for the interested reader.

Finally, (7d) is tested with

$$\underline{W}_{ni}^{3+} = (\underline{J}_{ni}^{3+})^* , \quad i = 1,2,...2M-3 \tag{30}$$

Substituting the expansions (19)-(21) into (7) and then testing (7) with (23), (24), (27), (28), and (30) in the previously described manner, we obtain the matrix equations

$$T_n \vec{X}_n = \vec{B}_n, \quad n = 0, \pm 1, \pm 2, \ldots \tag{31}$$

Here, $\vec{X}_n$ is a column vector of the unknown coefficients in (19)-(21). Also, T_n is a square matrix called the moment matrix. Finally, $\vec{B}_n$ is a column vector called the excitation vector. The elements of $\vec{B}_n$ are obtained by testing the known fields $\underline{E}^{i\pm}_{tan}$ and $\underline{H}^{i\pm}_{tan}$ on the right-hand sides of (7).

The column vector $\vec{X}_n$ is defined by

$$\tilde{X}_n = [\tilde{I}_n^{1+} \quad \tilde{I}_n^{1-} \quad \tilde{I}_n \quad \tilde{V}_n] \tag{32}$$

where the tilde (~) denotes the transpose of a column vector and where the jth elements of $\tilde{I}_n^{1+}$, $\tilde{I}_n^{1-}$, $\tilde{I}_n$, and $\tilde{V}_n$ are, respectively, I_{nj}^{1+}, I_{nj}^{1-}, I_{nj}, and V_{nj}.

The moment matrix T_n is given by

$$T_n = \begin{array}{|c|c|c|c|} \hline Z_n^{11+} & 0 & Z_n^{12+} & -Y_n^{13+} \\ \hline 0 & \eta_r Z_n^{11-} & \eta_r Z_n^{12-} & -Y_n^{13-} \\ \hline Z_n^{21+} & \eta_r Z_n^{21-} & Z_n^{22+} + \eta_r Z_n^{22-} & -Y_n^{23+} - Y_n^{23-} \\ \hline Y_n^{31+} & Y_n^{31-} & Y_n^{32+} + Y_n^{32-} & Z_n^{33+} + (\frac{1}{\eta_r}) Z_n^{33-} \\ \hline \end{array} \tag{33}$$

where

$$\eta_r = \frac{\eta^-}{\eta^+} \tag{34}$$

The ijth elements of the superscripted Z_n and Y_n submatrices in (33) are given by

$$Z_{nij}^{pq\pm} = -\langle W_{ni}^{p\pm}, \frac{1}{\eta^{\pm}} E^{\pm}(J_{nj}^{q\pm}, 0)\rangle \qquad p = 1,2,3 \qquad (35)$$

$$Y_{nij}^{pq+} = -\langle W_{ni}^{p\pm}, H^{+}(J_{nj}^{q\pm}, 0)\rangle \qquad q = 1,2,3 \qquad (36)$$

The new vector functions $\underline{J}_{nj}^{3-}$ and $\underline{W}_{ni}^{3-}$ unavoidably introduced in (35) and (36) are defined by

$$\left.\begin{aligned} \underline{J}_{nj}^{3-} &= \underline{J}_{nj}^{3+} \\ \underline{W}_{ni}^{3-} &= \underline{W}_{ni}^{3+} \end{aligned}\right\} \qquad (37)$$

No superscript "tan" is needed on the field operators $\underline{E}^{\pm}$ and $\underline{H}^{\pm}$ in (35) and (36) because the testing function $\underline{W}_{ni}^{p\pm}$ is tangential to the surface $(S^{+}+A)$. Because $\underline{W}_{ni}^{p\pm}$ and $\underline{J}_{nj}^{q\pm}$ have the dimension of (1/distance) and because the operators $\frac{1}{\eta^{\pm}} \underline{E}^{+}$ and $\underline{H}^{\pm}$ are dimensionless, expressions (35) and (36) are dimensionless. Hence, the elements of the moment matrix T_n are also dimensionless.

The excitation vector $\vec{B}_n$ in (31) is given by

$$\tilde{B}_n = [\tilde{V}_n^{il+} \quad \tilde{V}_n^{il-} \quad \tilde{V}_n^{i} \quad \tilde{I}_n^{i}] \qquad (38)$$

where the ith elements of $\tilde{V}_n^{il+}$, $\tilde{V}_n^{il-}$, $\tilde{V}_n^{i}$, and $\tilde{I}_n^{i}$ are given by

$$V_{ni}^{il+} = \langle W_{ni}^{l+}, \frac{1}{\eta^{+}} E^{i+}\rangle \qquad (39a)$$

$$V_{ni}^{il-} = -\langle W_{ni}^{l-}, \frac{1}{\eta^{+}} E^{i-}\rangle \qquad (39b)$$

$$V_{ni}^{i} = \langle W_{ni}^{2+}, \frac{1}{\eta^{+}} E^{i+}\rangle - \langle W_{ni}^{2-}, \frac{1}{\eta^{+}} E^{i-}\rangle \qquad (39c)$$

$$I_{ni}^{i} = \langle W_{ni}^{3+}, H^{i+}\rangle - \langle W_{ni}^{3+}, H^{i-}\rangle \qquad (39d)$$

The superscript i in (38) and (39) is not to be confused with the subscript i in (39). The former i indicates dependence on the fields $\underline{E}^{i\pm}$

and $\underline{H}^{i\pm}$. The latter i denotes the ith element of the column vector in question. No superscript "tan" is needed on $\underline{E}^{i\pm}$ and $\underline{H}^{i\pm}$ in (39) because all the testing functions in (39) are tangential vectors.

In general, the method of moments gives one matrix equation in which all the unknowns are coupled to each other. However, in the matrix equations (31) there is no coupling between $\vec{X}_n$ and $\vec{X}_m$ for $m \neq n$. This lack of coupling is a consequence of the nature of the field operators in (7), the $e^{jn\phi}$ dependence of the expansion functions, the $e^{-jn\phi}$ dependence of the testing functions, and the fact that the integral from 0 to 2π of the product of $e^{-jm\phi}$ with $e^{jn\phi}$ is zero whenever $m \neq n$. The two field operators which give the tangential electric and tangential magnetic fields due to an electric current appear in (7). An $e^{jn\phi}$ electric current produces an $e^{jn\phi}$ electric field [13, Appendix B] and an $e^{jn\phi}$ magnetic field [13, Eq. (9)]. In the previous sentence, the modifier $e^{jn\phi}$ means that the ϕ dependence is described by $e^{jn\phi}$. Actually, [13, Eq. (9)] represents the operator $-\underline{n} \times \underline{H}$ rather than $-\underline{H}$ where $\underline{H}$ denotes the magnetic field due to an electric current and $\underline{n}$ is the unit normal vector which points outward from the surface of the body of revolution in [13, Fig. 1]. However, the effect of $\underline{n}$ in $\underline{n} \times \underline{H}$ is to discard the normal component of $\underline{H}$ and to rotate the tangential component of $\underline{H}$ through an angle of 90° so that if $\underline{n} \times \underline{H}$ is $e^{jn\phi}$, then the tangential component of $\underline{H}$ is also $e^{jn\phi}$.

Equation (7d) can be called a magnetic field equation because it comes from the boundary condition that the tangential components of the magnetic field are continuous across the aperture. Since (7d) is a magnetic field equation, we were tempted to multiply it by $\underline{n}\times$ in order to make it conform to [13, Eq. (3)] and [14, Eq. (1)]. The $\underline{n}\times$ is vital to [14, Eq. (1)]. If the $\underline{n}\times$ were removed from [14, Eq. (1)], its method of moments solution using the testing and expansion functions defined in [14] would fail for any conducting body of revolution with a symmetric generating curve. The conducting sphere in [14, Fig. 1] is an example of a conducting body of revolution with a symmetric generating curve. The above mentioned failure of the method of moments may be due to the

fact that the magnetic field of an electric current is "cross polarized" with respect to the electric current. For example, the magnetic field of an electric current element is always perpendicular to that current element [7, Eq. (2-113)].

Although the $\underline{n} \times$ is vital to [14, Eq. (1)], we decided not to multiply (7d) by $\underline{n} \times$ because of the following two reasons.

1) The magnetic field in (7d) as it stands is not all cross polarized. Only the magnetic field due to the electric currents $\underline{J}^+ + \underline{I}$ is cross polarized. The magnetic field due to the magnetic current $\underline{M}$ is not cross polarized.

2) If (7d) were multiplied by $\underline{n} \times$, we would have to calculate matrix elements not only for the operators $\underline{E}^+(\underline{J},0)$ and $\underline{H}^+(\underline{J},0)$ but also for $\underline{n} \times \underline{E}^+(\underline{J},0)$ and $\underline{n} \times \underline{H}^+(\underline{J},0)$. If the functions which multiply $u_{t'}$ and $u_{\phi'}$ in (10) were the same, then the matrices for $\underline{n} \times \underline{E}^+(\underline{J},0)$ and $\underline{n} \times \underline{H}^+(\underline{J},0)$ could be obtained by merely rearranging the elements of the matrices for $\underline{E}^+(\underline{J},0)$ and $\underline{H}^+(\underline{J},0)$. Unfortunately, the function in (10b) is different from that in (10a) so that multiplication of (7d) by $\underline{n} \times$ would indeed require calculation of additional matrix elements.

According to (32), the solution of (31) for $\hat{X}_n$ determines the coefficients I'^+_{nj}, I^+_{nj}, and V^+_{nj} in (19)-(21). Thanks to (16), (17), and (22), expressions (19)-(21) for the electric and magnetic currents become

$$\underline{J}^+ + \underline{I} = \sum_{n=-\infty}^{\infty} \left[\sum_{j=1}^{M^+-1} I^{1+}_{nj} \underline{J}^{t+}_{nj} + \sum_{j=M^+}^{2M^+-1} I^{1+}_{nj} \underline{J}^{t+}_{n,j-M^++1} + \sum_{j=2M^+}^{N^++M^+-M-2} I^{1+}_{nj} \underline{J}^{t+}_{n,j-M^++M} \right.$$

$$\left. + \sum_{j=N^++M^+-M-1}^{2N^+-2M-2} I^{1+}_{nj} \underline{J}^{\phi+}_{n,j-N^++2M+1} + \sum_{j=1}^{M} I_{nj} \underline{J}^{t+}_{n,j+M^+-1} + \sum_{j=M+1}^{2M-1} I_{nj} \underline{J}^{\phi+}_{n,j+M^+-M} \right] \quad (40)$$

$$\underline{J}^{-}+\underline{J} = \sum_{n=-\infty}^{\infty}\left[\sum_{j=1}^{M^{-}-1} I^{1-}_{nj}J^{t-}_{nj} + \sum_{j=M^{-}}^{2M^{-}-1} I^{1-}_{nj}J^{\phi-}_{n,j-M^{-}+1} + \sum_{j=2M^{-}}^{N^{-}+M^{-}-M-2} I^{1-}_{nj}J^{t-}_{n,j-M^{-}+M}\right.$$

$$\left. + \sum_{j=N^{-}+M^{-}-M-1}^{2N^{-}-2M-3} I^{1-}_{nj}J^{\phi-}_{n,j-N^{-}+2M+1} + \sum_{j=1}^{M} I_{nj}J^{t-}_{n,j+M^{-}-1} + \sum_{j=M+1}^{2M-1} I_{nj}J^{\phi-}_{n,j+M^{-}-M}\right] \tag{41}$$

$$\underline{M} = \eta^{+}\sum_{n=-\infty}^{\infty}\left[\sum_{j=1}^{M-2} V_{nj}J^{t+}_{n,j+M^{+}} + \sum_{j=M-1}^{2M-3} V_{nj}J^{\phi+}_{n,j+M^{+}-M+2}\right] \tag{42}$$

IV. ELIMINATION OF T_n FOR NEGATIVE VALUES OF n

At first glance, solution of (31) requires calculation of the moment matrices T_n for both negative and non-negative values of n. However, we will show that each element of T_n is either even or odd in n. Consequently, by decomposing the excitation vector $\vec{B}_n$ into its even and odd parts with respect to n, we will be able to express the solutions to all of equations (31) in terms of the solutions to matrix equations involving only the moment matrices T_n for the non-negative values of n.

The equations and unknowns in (31) were ordered so that the moment matrix could, as in (33), be expressed in terms of a minimum number of submatrices. Unfortunately, the arrangement of equations and unknowns in (31) is not suitable for comparing the elements of T_{-n} with those of T_n. Hence, we rearrange the equations and unknowns in (31) to obtain

$$\begin{bmatrix} Z^{tt}_n & Z^{t\phi}_n & Y^{3tt}_n & Y^{3t\phi}_n \\ Z^{\phi t}_n & Z^{\phi\phi}_n & Y^{3\phi t}_n & Y^{3\phi\phi}_n \\ Y^{tt}_n & Y^{t\phi}_n & Z^{3tt}_n & Z^{3t\phi}_n \\ Y^{\phi t}_n & Y^{\phi\phi}_n & Z^{3\phi t}_n & Z^{3\phi\phi}_n \end{bmatrix} \begin{bmatrix} \vec{I}^{3t}_n \\ \vec{I}^{3\phi}_n \\ \vec{V}^{3t}_n \\ \vec{V}^{3\phi}_n \end{bmatrix} = \begin{bmatrix} \vec{V}^{i3t}_n \\ \vec{V}^{i3\phi}_n \\ \vec{I}^{i3t}_n \\ \vec{I}^{i3\phi}_n \end{bmatrix} \tag{43}$$

In (43), Z^{rs}_n, r being either t or ϕ and s being either t or ϕ, is the submatrix of all the elements of

$$\begin{bmatrix} Z_n^{11+} & 0 & Z_n^{12+} \\ 0 & \eta_r Z_n^{11-} & \eta_r Z_n^{12-} \\ Z_n^{21+} & \eta_r Z_n^{21-} & Z_n^{22+} + \eta_r Z_n^{22-} \end{bmatrix} \tag{44}$$

for which the testing function is r type and the expansion function is s type. Expression (44) was drawn from the right-hand side of (33). The testing functions $\underline{W}_{ni}^{p\pm}$ and expansion functions $\underline{J}_{nj}^{q\pm}$ enter (44) by means of (35). The s type expansion functions, s being either t or ϕ, are those on the right-hand sides of (16), (17) and (22) with the superscript s. The r type testing functions, r being either t or ϕ, are the complex conjugates of the r type expansion functions. Still in (43), Y_n^{rs}, r being either t or ϕ and s being either t or ϕ, is the submatrix of all the elements

$$[Y_n^{31+} \quad Y_n^{31-} \quad Y_n^{32+} + Y_n^{32-}]$$

for which the testing function is r type and the expansion function is s type. The submatrices Z_n^{3rs} and Y_n^{3rs} in (43) are similarly defined in terms of the remaining submatrices

$$[Z_n^{33+} + (\frac{1}{\eta_r})\ Z_n^{33-}]$$

and

$$\begin{bmatrix} -Y_n^{13+} \\ -Y_n^{13-} \\ -Y_n^{23+} - Y_n^{23-} \end{bmatrix}$$

on the right-hand side of (33).

The column vector $\underline{\tilde{I}}_n^{3s}$ in (43), s being either t or ϕ, consists of all the elements of

$$[\tilde{I}_n^{1+} \quad \tilde{I}_n^{1-}] \tag{45}$$

for which the superscript on the right-hand side of (18) is s and all the coefficients I_{nj} which multiply the s type expansion functions in (19). Expression (45) was drawn from (32). Similarly, $\vec{V}_n^{3s}$ in (43) is the column vector of all the coefficients of the s type expansion functions in (21).

The column vector $\vec{V}_n^{i3r}$ on the right-hand side of (43), r being either t or ϕ, consists of all the elements of

$$[\tilde{V}_n^{il+} \quad \tilde{V}_n^{il-} \quad \tilde{V}_n^{i}] \tag{46}$$

for which the testing function is r type. Expression (46) was drawn from (38). Finally, the column vector $\vec{I}_n^{i3r}$ in (43) consists of all the elements of $\tilde{I}_n^i$ for which the testing function is r type. The superscripts t and ϕ in (43) denote the types of testing and expansion functions. However, the superscript 3 in (43) has no special meaning. It serves only to distinguish matrices with it from those without it.

What happens to the submatrices Z_n^{rs} and Z_n^{3rs} on the left-hand side of (43) when n is replaced by -n? Previously, the elements of Z_n^{rs} and Z_n^{3rs} were traced back to those of the elements (35) for which the testing functions are r type and the expansion functions are s type. Thanks to (16), (17), (22), (23), (24), (27), (28), (30), and (37), the matrix element (35) can be written as

$$Z_{nij}^{pq+} = -\langle W_{ni'}^{r\pm}, \frac{1}{\eta^{\pm}} E^{+}(J_{nj'}^{s\pm}, 0)\rangle, \qquad \begin{cases} p = 1,2,3 \\ q = 1,2,3 \end{cases} \tag{47}$$

where $J_{nj'}^{s\pm}$ are the expansion functions appearing in (13) and (14) and

$$W_{ni'}^{r\pm} = (J_{ni'}^{r\pm})^{*} \tag{48}$$

The subscripts and superscripts on the left-hand side of (47) indicate the testing function $W_{ni}^{p\pm}$ and the expansion function $J_{nj}^{q\pm}$. It is understood from (35) that Z_{nij}^{pq+} indicates W_{ni}^{p+} and J_{nj}^{q+} and that Z_{nij}^{pq-} indicates W_{ni}^{p-} and J_{nj}^{q-}. In (47), r = t if $W_{ni}^{p\pm}$ is a t type expansion function,

and $r = \phi$ if $\underline{W}_{ni}^{p\pm}$ is a ϕ type expansion function. Similarly, s in (47) is determined by the type of the expansion function $\underline{J}_{nj}^{q\pm}$. According to (16), (17), and (22), the subscript j' in (47) is also determined by $\underline{J}_{nj}^{q\pm}$. Similarly, the subscript i' in (47) is determined by $\underline{W}_{ni}^{p\pm}$. Explicit expressions for i' and j' are not needed now. If the testing functions and expansion functions in [12, Eqs. (2)-(5)] are decorated by appending $\pm$ to their superscripts and by changing their subscripts i and j to i' and j' and if the normalized electric field operator $-\underline{E}^{s}/\eta$ used in [12] is replaced by $-\underline{E}^{\pm}/\eta^{\pm}$, then the elements of the moment matrix used in [12] will be coerced into becoming the right-hand side of (47).

The moment matrix used in [12] is given by [12, Eqs. (9)-(12)] from which it is evident that the tt and $\phi\phi$ submatrices are even in n and that the ϕt and tϕ submatrices are odd in n. Hence, the superscripted Z_n submatrices on the left-hand side of (43) satisfy

$$\begin{bmatrix} Z_{-n}^{tt} & Z_{-n}^{t\phi} \\ Z_{-n}^{\phi t} & Z_{-n}^{\phi\phi} \end{bmatrix} = \begin{bmatrix} Z_{n}^{tt} & -Z_{n}^{t\phi} \\ -Z_{n}^{\phi t} & Z_{n}^{\phi\phi} \end{bmatrix} \tag{49a}$$

$$\begin{bmatrix} Z_{-n}^{3tt} & Z_{-n}^{3t\phi} \\ Z_{-n}^{3\phi t} & Z_{-n}^{3\phi\phi} \end{bmatrix} = \begin{bmatrix} Z_{n}^{3tt} & -Z_{n}^{3t\phi} \\ -Z_{n}^{3\phi t} & Z_{n}^{3\phi\phi} \end{bmatrix} \tag{49b}$$

What happens to the submatrices Y_n^{rs} and Y_n^{3rs} on the left-hand side of (43) when n is replaced by -n? Previously, the elements of Y_n^{rs} and Y_n^{3rs} were traced back to those of the elements (36) for which the testing functions are r type and the expansion functions are s type. Replacement of $\underline{W}_{ni}^{p\pm}$ and $\underline{J}_{nj}^{q\pm}$ in (36) by $\underline{W}_{ni}^{r\pm}$, and $\underline{J}_{nj}^{s\pm}$, gives

$$Y_{nij}^{pq\pm} = -\langle \underline{W}_{ni'}^{r\pm}, , H^{\pm}(\underline{J}_{nj'}^{s\pm}, , 0)\rangle, \quad \begin{cases} p = 1,2,3 \\ q = 1,2,3 \end{cases} \tag{50}$$

The change in testing functions and expansion functions in going from (36) to (50) is the same as the change that sent (35) into (47).

If the testing functions and expansion functions in [14] are decorated by appending the superscript $^+$ and by changing their subscripts i and j to i' and j' and if the magnetic field operator $\underline{H}^s$ used in [14] is replaced by $\underline{H}^+$, then the elements of the moment matrix in [14] denoted by $Y^{rs^+}_{ni'j'}$, become

$$Y^{rs^+}_{ni'j'} = -\langle \underline{W}^{r^+}_{ni'}, \underline{n}^+ \times \underline{H}^+(\underline{J}^{s^+}_{nj'}, 0)\rangle \quad , \quad \begin{cases} r = t,\phi \\ s = t,\phi \end{cases} \tag{51}$$

where

$$\underline{n}^+ = \underline{u}_\phi \times \underline{u}_{t^+} \tag{52}$$

According to (52), $\underline{n}^+$ is a unit vector normal to the generating curve of $(S^+ + A)$. Although we have been omitting the vector designation from vectors inside the symmetric product, we decided to designate $\underline{n}^+$ and $\underline{H}^+$ as vectors in (51) to clearly indicate that the vector product $\underline{n}^+ \times \underline{H}^+$ is intended there. Striving toward (50), we rewrite (51) as

$$Y^{rs^+}_{ni'j'} = \langle \underline{n}^+ \times \underline{W}^{r^+}_{ni'}, H^+(\underline{J}^{s^+}_{nj'}, 0)\rangle, \quad \begin{cases} r = t,\phi \\ s = t,\phi \end{cases} \tag{53}$$

Modified testing functions $\hat{\underline{W}}^{r^+}_{ni'}$ are now defined by interchanging the t^+ and ϕ components of $\underline{W}^{r^+}_{ni'}$.

$$\hat{\underline{W}}^{t^+}_{ni'} = \underline{u}_{t^+}(\underline{W}^{\phi^+}_{ni'} \cdot \underline{u}_\phi) \tag{54a}$$

$$\hat{\underline{W}}^{\phi^+}_{ni'} = \underline{u}_\phi(\underline{W}^{t^+}_{ni'} \cdot \underline{u}_{t^+}) \tag{54b}$$

Replacement of $\underline{W}^{r^+}_{ni'}$ by $\hat{\underline{W}}^{r^+}_{ni'}$ in (53) gives

$$\hat{Y}^{rs\pm}_{ni'j'} = \langle \underline{n}^{\pm} \times \hat{\underline{W}}^{r\pm}_{ni'}, H^{\pm}(\underline{J}^{s\pm}_{nj'}, 0) \rangle, \quad \begin{cases} r = t,\phi \\ s = t,\phi \end{cases} \tag{55}$$

The symbol $\hat{}$ on the left-hand side of (55) indicates that the testing function is $\hat{\underline{W}}^{r\pm}_{ni'}$ instead of $\underline{W}^{r\pm}_{ni'}$. In view of (52) and (54), (55) becomes

$$\left.\begin{aligned} -\langle W^{t\pm}_{ni''}, H^{\pm}(J^{s\pm}_{nj''}, 0)\rangle &= -\hat{Y}^{\phi s\pm}_{ni'j'} \qquad (56a) \\ -\langle W^{\phi\pm}_{ni''}, H^{\pm}(J^{s\pm}_{nj''}, 0)\rangle &= \hat{Y}^{ts\pm}_{ni'j'} \qquad (56b) \end{aligned}\right\} \quad s = t,\phi$$

The left-hand sides of (56) are the r = t and r = ϕ portions of (50). Hence, (56) states that the r = t matrix element in (50) is the negative of the r = ϕ matrix element modified from [14] and that the r = ϕ matrix element in (50) is the r = t matrix element modified from [14]. The expression "matrix element modified from [14]" denotes the matrix element of [14] modified by replacing the testing function $\underline{W}^{r}_{ni}$ by $\hat{\underline{W}}^{r\pm}_{ni}$, of (54), replacing the expansion function $\underline{J}^{s}_{nj}$ by $\underline{J}^{s\pm}_{nj''}$, and replacing the magnetic field operator $\underline{H}^{s}$ by $\underline{H}^{\pm}$. Note that, since all Ampere's law contributions were suppressed in (3c) and (3d), the operator $\underline{H}^{\pm}$ does not contain any Ampere's law contribution.

It is evident from [14, Eq. (12)] that the tt and $\phi\phi$ matrix elements on the right-hand sides of (56) are even in n and that the ϕt and tϕ matrix elements on the right-hand sides of (56) are odd in n. Consequently, the tt and $\phi\phi$ matrix elements in (50) are odd in n and the ϕt and tϕ matrix elements in (50) are even in n. Hence, the submatrices Y^{rs}_{n} and Y^{3rs}_{n} on the left-hand side of (43) satisfy

$$\begin{bmatrix} Y^{tt}_{-n} & Y^{t\phi}_{-n} \\ Y^{\phi t}_{-n} & Y^{\phi\phi}_{-n} \end{bmatrix} = \begin{bmatrix} -Y^{tt}_{n} & Y^{t\phi}_{n} \\ Y^{\phi t}_{n} & -Y^{\phi\phi}_{n} \end{bmatrix} \tag{57a}$$

$$\begin{bmatrix} Y^{3tt}_{-n} & Y^{3t\phi}_{-n} \\ Y^{3\phi t}_{-n} & Y^{3\phi\phi}_{-n} \end{bmatrix} = \begin{bmatrix} -Y^{3tt}_{n} & Y^{3t\phi}_{n} \\ Y^{3\phi t}_{n} & -Y^{3\phi\phi}_{n} \end{bmatrix} \tag{57b}$$

Next, the excitation vector on the right-hand side of (43) is written as

$$\begin{bmatrix} \vec{V}_n^{i3t} \\ \vec{V}_n^{i3\phi} \\ \vec{I}_n^{i3t} \\ \vec{I}_n^{i3\phi} \end{bmatrix} = \begin{bmatrix} \vec{V}_n^{i3t\theta} \\ \vec{V}_n^{i3\phi\theta} \\ \vec{I}_n^{i3t\theta} \\ \vec{I}_n^{i3\phi\theta} \end{bmatrix} + \begin{bmatrix} \vec{V}_n^{i3t\phi} \\ \vec{V}_n^{i3\phi\phi} \\ \vec{I}_n^{i3t\phi} \\ \vec{I}_n^{i3\phi\phi} \end{bmatrix}, \quad n = 0, \pm 1, +2, \ldots \tag{58}$$

where

$$\begin{bmatrix} \vec{V}_n^{i3t\theta} \\ \vec{V}_n^{i3\phi\theta} \\ \vec{I}_n^{i3t\theta} \\ \vec{I}_n^{i3\phi\theta} \end{bmatrix} = \frac{1}{2} \begin{bmatrix} \vec{V}_n^{i3t} + \vec{V}_{-n}^{i3t} \\ \vec{V}_n^{i3\phi} - \vec{V}_{-n}^{i3\phi} \\ \vec{I}_n^{i3t} - \vec{I}_{-n}^{i3t} \\ \vec{I}_n^{i3\phi} + \vec{I}_{-n}^{i3\phi} \end{bmatrix} \tag{59a}$$

$$\begin{bmatrix} \vec{V}_n^{i3t\phi} \\ \vec{V}_n^{i3\phi\phi} \\ \vec{I}_n^{i3t\phi} \\ \vec{I}_n^{i3\phi\phi} \end{bmatrix} = \frac{1}{2} \begin{bmatrix} \vec{V}_n^{i3t} - \vec{V}_{-n}^{i3t} \\ \vec{V}_n^{i3\phi} + \vec{V}_{-n}^{i3\phi} \\ \vec{I}_n^{i3t} + \vec{I}_{-n}^{i3t} \\ \vec{I}_n^{i3\phi} - \vec{I}_{-n}^{i3\phi} \end{bmatrix} \tag{59b}$$

The last superscript θ or ϕ on the column vectors on the right-hand side of (58) distinguishes those column vectors from each other and from the excitation vector on the left-hand side of (58). For a particular value of n, the solution to (43) is the sum of the solutions obtained by replacing the excitation vector by (59a) and (59b) successively. Hence, we write

$$\begin{bmatrix} \vec{I}_n^{3t} \\ \vec{I}_n^{3\phi} \\ \vec{V}_n^{3t} \\ \vec{V}_n^{3\phi} \end{bmatrix} = \begin{bmatrix} \vec{I}_n^{3t\theta} \\ \vec{I}_n^{3\phi\theta} \\ \vec{V}_n^{3t\theta} \\ \vec{V}_n^{3\phi\theta} \end{bmatrix} + \begin{bmatrix} \vec{I}_n^{3t\phi} \\ \vec{I}_n^{3\phi\phi} \\ \vec{V}_n^{3t\phi} \\ \vec{V}_n^{3\phi\phi} \end{bmatrix} \tag{60}$$

where the column vectors on right-hand side of (60) satisfy

$$\begin{bmatrix} Z_n^{tt} & Z_n^{t\phi} & Y_n^{3tt} & Y_n^{3t\phi} \\ Z_n^{\phi t} & Z_n^{\phi\phi} & Y_n^{3\phi t} & Y_n^{3\phi\phi} \\ Y_n^{tt} & Y_n^{t\phi} & Z_n^{3tt} & Z_n^{3t\phi} \\ Y_n^{\phi t} & Y_n^{\phi\phi} & Z_n^{3\phi t} & Z_n^{3\phi\phi} \end{bmatrix} \begin{bmatrix} \vec{I}_n^{3tu} \\ \vec{I}_n^{3\phi u} \\ \vec{V}_n^{3tu} \\ \vec{V}_n^{3\phi u} \end{bmatrix} = \begin{bmatrix} \vec{V}_n^{i3tu} \\ \vec{V}_n^{i3\phi u} \\ \vec{I}_n^{i3tu} \\ \vec{I}_n^{i3\phi u} \end{bmatrix}, \quad u = \theta,\phi \qquad (61)$$

It is evident from (59) that

$$[V_{-n}^{i3t\theta} \quad V_{-n}^{i3\phi\theta} \quad I_{-n}^{i3t\theta} \quad I_{-n}^{i3\phi\theta}] = [\tilde{V}_n^{i3t\theta} \quad -\tilde{V}_n^{i3\phi\theta} \quad -\tilde{I}_n^{i3t\theta} \quad \tilde{I}_n^{i3\phi\theta}] \qquad (62a)$$

$$[V_{-n}^{i3t\phi} \quad V_{-n}^{i3\phi\phi} \quad I_{-n}^{i3t\phi} \quad I_{-n}^{i3\phi\phi}] = [-\tilde{V}_n^{i3t\phi} \quad \tilde{V}_n^{i3\phi\phi} \quad \tilde{I}_n^{i3t\phi} \quad -\tilde{I}_n^{i3\phi\phi}] \qquad (62b)$$

If n is replaced by -n in (61), and if (49), (57), and (62) are substituted for the -n submatrices and excitation vectors, then comparison of the resulting matrix equation with (61) yields

$$[I_{-n}^{3t\theta} \quad I_{-n}^{3\phi\theta} \quad V_{-n}^{3t\theta} \quad V_{-n}^{3\phi\theta}] = [\tilde{I}_n^{3t\theta} \quad -\tilde{I}_n^{3\phi\theta} \quad -\tilde{V}_n^{3t\theta} \quad \tilde{V}_n^{3\phi\theta}] \qquad (63a)$$

$$[I_{-n}^{3t\phi} \quad I_{-n}^{3\phi\phi} \quad V_{-n}^{3t\phi} \quad V_{-n}^{3\phi\phi}] = [-\tilde{I}_n^{3t\phi} \quad \tilde{I}_n^{3\phi\phi} \quad \tilde{V}_n^{3t\phi} \quad -\tilde{V}_n^{3\phi\phi}] \qquad (63b)$$

The solution to (43) is now given by (60) where the column vectors for non-negative values of n on the right-hand side of (60) are obtained by solving (61) and the column vectors for negative values of n are given by (63).

The result stated in the previous sentence concerning the solution to (43) will eventually be applied to the solution to (31). The solution $\vec{X}_n$ to (31) is written as

$$\vec{X}_n = \vec{X}_n^{\theta} + \vec{X}_n^{\phi} \qquad (64)$$

where, for non-negative values of n, $\vec{X}_n^{\theta}$ and $\vec{X}_n^{\phi}$ are obtained by solving

$$T_n \vec{X}_n^{\theta} = \vec{B}_n^{\theta} \qquad (65a)$$

$$T_n \vec{X}_n^{\phi} = \vec{B}_n^{\phi} \qquad (65b)$$

where

$$\tilde{B}_n^{\theta} = [\tilde{V}_n^{il+\theta} \quad \tilde{V}_n^{il-\theta} \quad \tilde{V}_n^{i\theta} \quad \tilde{I}_n^{i\theta}] \tag{66a}$$

$$\tilde{B}_n^{\phi} = [\tilde{V}_n^{il+\phi} \quad \tilde{V}_n^{il-\phi} \quad \tilde{V}_n^{i\phi} \quad \tilde{I}_n^{i\phi}] \tag{66b}$$

where

$$\begin{bmatrix} \vec{V}_n^{il+\theta} \\ \vec{V}_n^{il-\theta} \\ \vec{V}_n^{i\theta} \\ \vec{I}_n^{i\theta} \end{bmatrix} = \frac{1}{2} \begin{bmatrix} \vec{V}_n^{il+} & \pm & \vec{V}_{-n}^{il+} \\ \vec{V}_n^{il-} & \pm & \vec{V}_{-n}^{il-} \\ \vec{V}_n^{i} & \pm & \vec{V}_{-n}^{i} \\ \vec{I}_n^{i} & \mp & \vec{I}_{-n}^{i} \end{bmatrix} \tag{67a}$$

$$\begin{bmatrix} \vec{V}_n^{il+\phi} \\ \vec{V}_n^{il-\phi} \\ \vec{V}_n^{i\phi} \\ \vec{I}_n^{i\phi} \end{bmatrix} = \frac{1}{2} \begin{bmatrix} \vec{V}_n^{il+} & \mp & \vec{V}_{-n}^{il+} \\ \vec{V}_n^{il-} & \mp & \vec{V}_{-n}^{il-} \\ \vec{V}_n^{i} & \mp & \vec{V}_{-n}^{i} \\ \vec{I}_n^{i} & \pm & \vec{I}_{-n}^{i} \end{bmatrix} \tag{67b}$$

The elements of the column vectors on the right-hand sides of (67) are given by (39). In the same way that $\underline{W}_{ni}^{p\pm}$, p=1,2,3, in (35) was replaced by $\underline{W}_{ni}^{r+}$, in order to obtain (47), the testing function $\underline{W}_{ni}^{p+}$ in (39) can be replaced by $\underline{W}_{ni}^{r+}$,. On the right-hand sides of (67), the upper sign applies to elements for which the testing function in (39) is t type and the lower sign applies when the testing function is ϕ type.

We wish to express the currents (40)-(42) in terms of the elements of $\vec{X}_n^{t}$ and $\vec{X}_n^{\phi}$ for non-negative values of n. With this objective in mind and taking a cue from (64), we separate (32) into

$$\tilde{X}_n^{\theta} = [\tilde{I}_n^{1+\theta} \quad \tilde{I}_n^{1-\theta} \quad \tilde{I}_n^{\theta} \quad \tilde{V}_n^{\theta}] \tag{68a}$$

$$\tilde{X}_n^{\phi} = [\tilde{I}_n^{1+\phi} \quad \tilde{I}_n^{1-\phi} \quad \tilde{I}_n^{\phi} \quad \tilde{V}_n^{\phi}] \tag{68b}$$

In view of (68), the currents (40)-(42) become

$$\underline{J}^{+}+\underline{J} = (\underline{J}^{+\theta} + \underline{J}^{\theta}) + (\underline{J}^{+\phi} + \underline{J}^{\phi}) \tag{69}$$

$$\underline{J}^{-}+\underline{J} = (\underline{J}^{-\theta} + \underline{J}^{\theta}) + (\underline{J}^{-\phi} + \underline{J}^{\phi}) \tag{70}$$

$$\underline{M} = \underline{M}^{\theta} + \underline{M}^{\phi} \tag{71}$$

where the currents with the superscript θ on the right-hand sides of (69)-(71) are due to the set of all the $\tilde{X}_n^{\theta}$'s for all values of n. Similarly, the currents with the superscript ϕ are due to the $\tilde{X}_n^{\phi}$'s. More explicitly, $(\underline{J}^{+u} + \underline{J}^{u})$, u being either θ or ϕ, is given by (40) with I_{nj}^{1+} and I_{nj} replaced by I_{nj}^{1+u} and I_{nj}^{u}, respectively. Here, I_{nj}^{1+u} and I_{nj}^{u} are the jth elements of $\tilde{I}_n^{1+u}$ and $\tilde{I}_n^{u}$, respectively. Likewise, $(\underline{J}^{-u} + \underline{J}^{u})$ is given by (41) with I_{nj}^{1-} and I_{nj} replaced by the jth elements I_{nj}^{1-u} and I_{nj}^{u} of $\tilde{I}_n^{1-u}$ and $\tilde{I}_n^{u}$. Finally, $\underline{M}^{u}$ is given by (42) with V_{nj} replaced by the jth element V_{nj}^{u} of $\tilde{V}_n^{u}$.

In view of (63),

$$\tilde{X}_{-n}^{\theta} = [+\tilde{I}_n^{1+\theta} \pm \tilde{I}_n^{1-\theta} \pm \tilde{I}_n^{\theta} \mp \tilde{V}_n^{\theta}] \tag{72a}$$

$$\tilde{X}_{-n}^{\phi} = [+\tilde{I}_n^{1+\phi} \mp \tilde{I}_n^{1-\phi} \mp \tilde{I}_n^{\phi} \pm \tilde{V}_n^{\phi}] \tag{72b}$$

where the upper sign applies to the coefficients of the t type expansion functions in (40)-(42) and the lower sign applies to the coefficients of the ϕ type expansion functions in (40)-(42). Thanks to (72) and (10), the t and ϕ components of the currents on the right-hand sides of (69)-(71) become

$$(\underline{J}^{+\theta} + \underline{J}^{\theta}) \cdot \underline{u}_{t+} = k^{+} \sum_{n=0}^{\infty} J_n^{t+\theta} \cos(n\phi) \tag{73a}$$

$$(\underline{J}^{+\theta} + \underline{J}^{\theta}) \cdot \underline{u}_{\phi} = k^{+} \sum_{n=1}^{\infty} J_n^{\phi+\theta} \sin(n\phi) \tag{73b}$$

$$(\underline{J}^{-\theta} + \underline{J}^{\theta}) \cdot \underline{u}_{t-} = k^{+} \sum_{n=0}^{\infty} J_n^{t-\theta} \cos(n\phi) \tag{74a}$$

$$(\underline{J}^{-\theta} + \underline{J}^{\theta}) \cdot \underline{u}_{\phi} = k^{+} \sum_{n=1}^{\infty} J_n^{\phi-\theta} \sin(n\phi) \tag{74b}$$

$$\underline{M}^{\theta} \cdot \underline{u}_{t+} = k^{+}\eta^{+} \sum_{n=1}^{\infty} M_n^{t\theta} \sin(n\phi) \tag{75a}$$

$$\underline{M}^{\theta} \cdot \underline{u}_{\phi} = k^{+}\eta^{+} \sum_{n=0}^{\infty} M_n^{\phi\theta} \cos(n\phi) \tag{75b}$$

$$(\underline{J}^{+\phi} + \underline{J}^{\phi}) \cdot \underline{u}_{t+} = k^{+} \sum_{n=1}^{\infty} J_n^{t+\phi} \sin(n\phi) \tag{76a}$$

$$(\underline{J}^{+\phi} + \underline{J}^{\phi}) \cdot \underline{u}_{\phi} = k^{+} \sum_{n=0}^{\infty} J_n^{\phi+\phi} \cos(n\phi) \tag{76b}$$

$$(\underline{J}^{-\phi} + \underline{J}^{\phi}) \cdot \underline{u}_{t-} = k^{+} \sum_{n=1}^{\infty} J_n^{t-\phi} \sin(n\phi) \tag{77a}$$

$$(\underline{J}^{-\phi} + \underline{J}^{\phi}) \cdot \underline{u}_{\phi} = k^{+} \sum_{n=0}^{\infty} J_n^{\phi-\phi} \cos(n\phi) \tag{77b}$$

$$\underline{M}^{\phi} \cdot \underline{u}_{t+} = k^{+}\eta^{+} \sum_{n=0}^{\infty} M_n^{t\phi} \cos(n\phi) \tag{78a}$$

$$\underline{M}^{\phi} \cdot \underline{u}_{\phi} = k^{+}\eta^{+} \sum_{n=1}^{\infty} M_n^{\phi\phi} \sin(n\phi) \tag{78b}$$

where

$$J_n^{t+\theta} = \varepsilon_n \left[\sum_{j=1}^{M^+-1} I_{nj}^{1+\theta} \left(\frac{T_j^+(t^+)}{k^+\rho^+} \right) + \sum_{j=M^+}^{M^++M-1} I_{n,j-M^++1}^{\theta} \left(\frac{T_j^+(t^+)}{k^+\rho^+} \right) + \sum_{j=M^++M}^{N^+-2} I_{n,j+M^+-M}^{1+\theta} \left(\frac{T_j^+(t^+)}{k^+\rho^+} \right) \right] \tag{79a}$$

$$J_n^{\phi+\theta} = 2j \left[\sum_{j=1}^{M^+} I_{n,j+M^+-1}^{1+\theta} \left(\frac{P_j^+(t^+)}{k^+\rho_j^+} \right) + \sum_{j=M^++1}^{M^++M-1} I_{n,j-M^++M}^{\theta} \left(\frac{P_j^+(t^+)}{k^+\rho_j^+} \right) + \sum_{j=M^++M}^{N^+-1} I_{n,j+N^+-2M-1}^{1+\theta} \left(\frac{P_j^+(t^+)}{k^+\rho_j^+} \right) \right] \tag{79b}$$

$$J_n^{t-\theta} = \varepsilon_n \left[\sum_{j=1}^{M^--1} I_{nj}^{1-\theta} \left(\frac{T_j^-(t^-)}{k^+\rho^-} \right) + \sum_{j=M^-}^{M^-+M-1} I_{n,j-M^-+1}^{\theta} \left(\frac{T_j^-(t^-)}{k^+\rho^-} \right) + \sum_{j=M^-+M}^{N^--2} I_{n,j+M^--M}^{1-\theta} \left(\frac{T_j^-(t^-)}{k^+\rho^-} \right) \right] \tag{80a}$$

$$J_n^{\phi-\theta} = 2j \left[\sum_{j=1}^{M^-} I_{n,j+M^--1}^{1-\theta} \left(\frac{P_j^-(t^-)}{k^+\rho_j^-} \right) + \sum_{j=M^-+1}^{M^-+M-1} I_{n,j-M^-+M}^{\theta} \left(\frac{P_j^-(t^-)}{k^+\rho_j^-} \right) + \sum_{j=M^-+M}^{N^--2} I_{n,j+N^--2M-1}^{1-\theta} \left(\frac{P_j^-(t^-)}{k^+\rho_j^-} \right) \right] \tag{80b}$$

$$M_n^{t\theta} = 2j \left[\sum_{j=M^++1}^{M^++M-2} V_{n,j-M^+}^{\theta} \left(\frac{T_j^+(t^+)}{k^+\rho^+} \right) \right] \tag{81a}$$

$$M_n^{\phi\theta} = \varepsilon_n \left[\sum_{j=M^++1}^{M^++M-1} V_{n,j-M^++M-2}^{\theta} \left(\frac{P_j^+(t^+)}{k^+\rho_j^+} \right) \right] \tag{81b}$$

$$J_n^{t+\phi} = 2j\left[\sum_{j=1}^{M^+-1} I_{nj}^{1+\phi}\left(\frac{T_j^+(t^+)}{k^+\rho^+}\right) + \sum_{j=M^+}^{M^++M-1} I_{n,j-M^++1}^{\phi}\left(\frac{T_j^+(t^+)}{k^+\rho^+}\right)\right.$$

$$\left. + \sum_{j=M^++M}^{N^+-2} I_{n,j+M^+-M}^{1+\phi}\left(\frac{T_j^+(t^+)}{k^+\rho^+}\right)\right] \qquad (82a)$$

$$J_n^{\phi+\phi} = \varepsilon_n\left[\sum_{j=1}^{M^+} I_{n,j+M^+-1}^{1+\phi}\left(\frac{P_j^+(t^+)}{k^+\rho_j^+}\right) + \sum_{j=M^++1}^{M^++M-1} I_{n,j-M^++M}^{\phi}\left(\frac{P_j^+(t^+)}{k^+\rho_j^+}\right)\right.$$

$$\left. + \sum_{j=M^++M}^{N^+-1} I_{n,j+N^+-2M-1}^{1+\phi}\left(\frac{P_j^+(t^+)}{k^+\rho_j^+}\right)\right] \qquad (82b)$$

$$J_n^{t-\phi} = 2j\left[\sum_{j=1}^{M^--1} I_{nj}^{1-\phi}\left(\frac{T_j^-(t^-)}{k^+\rho^-}\right) + \sum_{j=M^-}^{M^-+M-1} I_{n,j-M^-+1}^{\phi}\left(\frac{T_j^-(t^-)}{k^+\rho^-}\right)\right.$$

$$\left. + \sum_{j=M^-+M}^{N^--2} I_{n,j+M^--M}^{1-\phi}\left(\frac{T_j^-(t^-)}{k^+\rho_j^-}\right)\right] \qquad (83a)$$

$$J_n^{\phi-\phi} = \varepsilon_n\left[\sum_{j=1}^{M^-} I_{n,j+M^--1}^{1-\phi}\left(\frac{P_j^-(t^-)}{k^+\rho_j^-}\right) + \sum_{j=M^-+1}^{M^-+M-1} I_{n,j-M^-+M}^{\phi}\left(\frac{P_j^-(t^-)}{k^+\rho_j^-}\right)\right.$$

$$\left. + \sum_{j=M^-+M}^{N^--2} I_{n,j+N^--2M-1}^{1-\phi}\left(\frac{P_j^-(t^-)}{k^+\rho_j^-}\right)\right] \qquad (83b)$$

$$M_n^{t\phi} = \varepsilon_n\left[\sum_{j=M^++1}^{M^++M-2} V_{n,j-M^+}^{\phi}\left(\frac{T_j^+(t^+)}{k^+\rho^+}\right)\right] \qquad (84a)$$

$$M_n^{\phi\phi} = 2j\left[\sum_{j=M^++1}^{M^++M-1} V_{n,j-M^++M-2}^{\phi}\left(\frac{P_j^+(t^+)}{k^+\rho_j^+}\right)\right] \qquad (84b)$$

where

$$\varepsilon_n = \begin{cases} 1 & n = 0 \\ 2 & n > 0 \end{cases} \tag{85}$$

In (73)-(84), k^+ is the propagation constant in the medium characterized by (μ^+, ϵ^+). At present, placement of the factor k^+ in (73)-(78) and the factor $1/k^+$ in (79)-(84) can only be viewed as a matter of choice. The j that appears in the factor 2j which alternates with ε_n in (79)-(84) is $\sqrt{-1}$. The rest of the j's in (79)-(84) are summation indices.

Because of the subsectional nature of the triangle functions, only one of them, namely $T^+_{j-1}(t^+)$, contributes to (79a) when $t^+ = \bar{t}^+_j$ where j-1 is one possible value of any of the summation indices in (79a). Similar results can be stated for (80a) and (81a). The pulse function $P^{\pm}_j(t^{\pm})$ is centered at $t^+ = t^+_j$ where

$$t^+_j = \frac{1}{2}\,(\bar{t}^+_j + \bar{t}^+_{j+1}) \tag{86}$$

Because of the subsectional nature of the pulse functions, only one of them contributes to (79b) when $t^+ = t^+_j$ where j is one possible value of any of the summation indices in (79b). Similar results can be stated for (80b) and (81b). Hence, the values of (79)-(81) at the peaks of the triangle functions and at the centers of the pulse functions are given by

$$J^{t+0}_n(\bar{t}^+_j) = \begin{cases} \dfrac{\varepsilon_n I^{1+0}_{n1}}{k^{+-+}\rho_2} & j = 1 \\ \dfrac{\varepsilon_n I^{1+0}_{n,j-1}}{k^{+-+}\rho_j} & j = 2,3,\ldots M^+ \\ \dfrac{\varepsilon_n I^{0}_{n,j-M^+}}{k^{+-+}\rho_j} & j = M^+{+}1,\ M^+{+}2,\ldots M^+{+}M \\ \dfrac{\varepsilon_n I^{1+0}_{n,j+M^+-M-1}}{k^{+-+}\rho_j} & j = M^+{+}M{+}1,\ M^+{+}M{+}2,\ldots N^+{-}1 \\ \dfrac{\varepsilon_n I^{1+0}_{n,N^+-M^+-M-2}}{k^{+-+}\rho_{N^+-1}} & j = N^+ \end{cases} \tag{87a}$$

$$J_n^{\phi+\theta}(t_j^+) = \begin{cases} \dfrac{2jI^{1+\theta}_{n,j+M^+-1}}{k^+\rho_j^+} & j = 1,2,\ldots M^+ \\ \dfrac{2jI^{\theta}_{n,j-M^++M}}{k^+\rho_j^+} & j = M^++1,\ M^++2,\ldots M^++M-1 \\ \dfrac{2jI^{1+\theta}_{n,j+N^+-2M-1}}{k^+\rho_j^+} & j = M^++M,\ M^++M+1,\ldots N^+-1 \end{cases} \tag{87b}$$

$$J_n^{t-\theta}(\bar{t}_j^-) = \begin{cases} \dfrac{\varepsilon_n I^{1-\theta}_{n,j-1}}{k^+\bar{\rho}_j^-} & j = 2,3,\ldots M^- \\ \dfrac{\varepsilon_n I^{\theta}_{n,j-M^-}}{k^+\bar{\rho}_j^-} & j = M^-+1,\ M^-+2,\ldots M^-+M \\ \dfrac{\varepsilon_n I^{1-\theta}_{n,j+M^--M-1}}{k^+\bar{\rho}_j^-} & j = M^-+M+1,\ M^-+M+2,\ldots N^--1 \end{cases} \tag{88a}$$

$$J_n^{\phi-\theta}(t_j^-) = \begin{cases} \dfrac{2jI^{1-\theta}_{n,j+M^--1}}{k^+\rho_j^-} & j = 1,2,\ldots M^- \\ \dfrac{2jI^{\theta}_{n,j-M^-+M}}{k^+\rho_j^-} & j = M^-+1,\ M^-+2,\ldots M^-+M-1 \\ \dfrac{2jI^{1-\theta}_{n,j+N^--2M-1}}{k^+\rho_j^-} & j = M^-+M,\ M^-+M+1,\ldots N^--2 \end{cases} \tag{88b}$$

$$M_n^{t\theta}(\bar{t}_j^+) = \begin{cases} 0 & j = M^+ + 1 \\ \dfrac{2jV^{\theta}_{n,j-M^+-1}}{k^+\rho_j^{-+}} & j = M^+ + 2,\ M^+ + 3, \ldots M^+ + M - 1 \\ 0 & j = M^+ + M \end{cases} \qquad (89a)$$

$$M_n^{t\phi}(t_j^+) = \frac{\epsilon_n V^{\phi}_{n,j-M^+ + M-2}}{k^+ \rho_j^+} \qquad j = M^+ + 1,\ M^+ + 2, \ldots M^+ + M + 1 \qquad (89b)$$

The non-zero values of $J_n^{t+\theta}$ stated at $\bar{t}_1^+$ and $\bar{t}_{N^+}^+$ in (87a) are due not to peaks of triangle functions but to the fact that $\bar{t}_1^+$ and $\bar{t}_{N^+}^+$ lie on the z axis. These non-zero values were established in the paragraph which follows the one containing (12). The starting and finishing values of zero were included in (89a) to emphasize the fact that $M_n^{t\theta}$ goes to zero at the edges of the aperture.

The values of (82)-(84) at the peaks of the triangle functions and at the centers of the pulse functions are not written here. It suffices to say that these values are given by the right-hand sides of (87)-(89) with the factors ϵ_n and 2j interchanged and with the superscript θ replaced by ϕ.

In summary, the electric and magnetic currents are given by (69)-(71) and (73)-(84) of which (79)-(81) specialize to (87)-(89). According to (68), the I's and V's in (79)-(84) are elements of $\vec{X}_n^{\theta}$ and $\vec{X}_n^{\phi}$. Now, $\vec{X}_n^{\theta}$ and $\vec{X}_n^{\phi}$ are obtained by solving (65) for non-negative values of n. The moment matrices T_n in (65) are given by (33)-(36). However, (35) was reduced to (47) and (36) was reduced to the combination of (50) and (56). The excitation vectors $\vec{B}_n^{\theta}$ and $\vec{B}_n^{\phi}$ in (65) are given by (66), (67), and (39) or rather (39) with W_{ni}^{p+}, p = 1,2,3, replaced by W_{ni}^{r-}.

V. PLANE WAVE INCIDENCE

In this section, the method of moments solution summarized in the last paragraph of Section IV is specialized to the case in which $(\underline{E}^{i+}, \underline{H}^{i+})$ is an obliquely incident plane wave and $\underline{E}^{i-} = \underline{H}^{i-} = 0$. If the excitation $(\underline{E}^{i+}, \underline{H}^{i+})$ is rotated in ϕ by an angle ϕ_o, then it is evident from rotational symmetry that the response will rotate by the same angle ϕ_o. Hence, we may, without loss of generality, assume that the propagation vector of the incident plane wave lies in the xz plane. Any plane wave can be written as the sum of a θ-polarized plane wave and a ϕ-polarized plane wave. Thus, it suffices to solve the electromagnetic problem first for a θ-polarized incident plane wave and then for a ϕ-polarized incident plane wave.

For the θ-polarized incident plane wave, we choose

$$(\underline{E}^{i+}, \underline{H}^{i+}) = (\underline{E}^{\theta}, \underline{H}^{\theta}) \tag{90a}$$

where

$$\underline{E}^{\theta} = \underline{u}_{\theta}^{t} \, k^{+} \eta^{+} e^{-j\underline{k}_t \cdot \underline{r}} \tag{90b}$$

$$\underline{H}^{\phi} = - \underline{u}_{\phi}^{t} k^{+} e^{-j\underline{k}_t \cdot \underline{r}} \tag{90c}$$

The ϕ-polarized incident plane wave is defined by

$$(\underline{E}^{i+}, \underline{H}^{i+}) = (\underline{E}^{\phi}, \underline{H}^{\phi}) \tag{91a}$$

where

$$\underline{E}^{\phi} = \underline{u}_{\phi}^{t} k^{+} \eta^{+} e^{-j\underline{k}_t \cdot \underline{r}} \tag{91b}$$

$$\underline{H}^{\phi} = \underline{u}_{\theta}^{t} k^{+} e^{-j\underline{k}_t \cdot \underline{r}} \tag{91c}$$

In (90) and (91), $\underline{r}$ is the radius vector from the origin, and $\underline{k}_t$ is the propagation vector given by

$$\underline{k}_t = - k^{+} (\underline{u}_x \sin \theta_t + \underline{u}_z \cos \theta_t) \tag{92}$$

Also, $\underline{u}_{\theta}^{t}$ and $\underline{u}_{\phi}^{t}$ are unit vectors given by

$$\underline{u}_{\theta}^{t} = \underline{u}_x \cos \theta_t - \underline{u}_z \sin \theta_t \tag{93a}$$

$$\underline{u}_{\phi}^{t} = \underline{u}_y \tag{93b}$$

In (92) and (93), $\underline{u}_x$, $\underline{u}_y$, and $\underline{u}_z$ are unit vectors in the x,y, and z directions, respectively. The "t" in (92) and (93) stands for transmitter. Presumably, each of the incident waves (90) and (91) is produced by a distant transmitter. According to (92), the transmitter bearing is given by $(\theta,\phi) = (\theta_t, 0)$ where θ is the angle that the radius vector from the origin makes with the positive z axis. When $(\theta,\phi) = (\theta_t, 0)$, $\underline{u}_{\theta}^{t}$ and $\underline{u}_{\phi}^{t}$ coincide with the unit vectors in the θ and ϕ directions, respectively.

The excitation vectors B_n^{i+} and B_n^{i-} of (66) are now obtained for the θ-polarized wave (90). Replacement of $\underline{W}_{ni}^{p+}$, p = 1,2,3, by $\underline{W}_{ni}^{r+}$, in (39) and substitution of (90) and (0,0) for $(\underline{E}^{i+}, \underline{H}^{i+})$ and $(\underline{E}^{i-}, \underline{H}^{i-})$ in (39) yield

$$V_{ni}^{il+} = \langle \underline{W}_{ni'}^{r+}, \frac{1}{\eta^+} E^{\theta} \rangle \tag{94a}$$

$$V_{ni}^{il-} = 0 \tag{94b}$$

$$V_{ni}^{i} = \langle \underline{W}_{ni'}^{r+}, \frac{1}{\eta^+} E^{\theta} \rangle \tag{94c}$$

$$I_{ni}^{i} = \langle \underline{W}_{ni'}^{r+}, H^{\theta} \rangle \tag{94d}$$

The values of r and i' in (94a) depend on $\underline{W}_{ni}^{1+}$, the values of r and i' in (94c) depend on $\underline{W}_{ni}^{2+}$, and the values of r and i' in (94d) depend on $\underline{W}_{ni}^{3+}$. It is evident from (90c) and (91b) that $H^{\theta} = -\underline{E}^{\phi}/\eta^+$ so that (94) becomes

$$V_{ni}^{il+} = \langle \underline{W}_{ni'}^{r+}, \frac{1}{\eta^+} E^{\theta} \rangle \tag{95a}$$

$$V_{ni}^{il-} = 0 \tag{95b}$$

$$V_{ni}^{i} = \langle \underline{W}_{ni'}^{r+}, \frac{1}{\eta^+} E^{\theta} \rangle \tag{95c}$$

$$I_{ni}^{i} = -\langle \underline{W}_{ni'}^{r+}, \frac{1}{\eta^+} E^{\phi} \rangle \tag{95d}$$

Now, (95) reduces to

$$V_{ni}^{il+} = V_{ni'}^{r\theta} \tag{96a}$$

$$V_{ni}^{il-} = 0 \tag{96b}$$

$$V_{ni}^{i} = V_{ni'}^{r\theta} \tag{96c}$$

$$I_{ni}^{i} = - V_{ni'}^{r\phi} \tag{96d}$$

where the V's on the right-hand sides of (96) are given by [12, Eqs. (113), (114), (116), and (117)] with i replaced by i', k replaced by k^+, and the quantities in the integrands made appropriate to the generating curve of $(S^+ + A)$. The reader should not be misled into believing that the right-hand sides of (96a) and (96c) are equal to each other. Because r and i' originated in (94), their values in (96c) are not necessarily the same as those in (96a).

With regard to the right-hand sides of (96), it is evident from [12] that $V_{ni'}^{t\theta}$, and $V_{ni'}^{\phi\phi}$, are even in n and that $V_{ni'}^{\phi\theta}$, and $V_{ni'}^{t\phi}$, are odd in n. Hence, substitution of (96) into (67) with due regard to (66) gives

$$\tilde{B}_n^{\theta} = [\tilde{V}_n^{il+} \quad 0 \quad \tilde{V}_n^{i} \quad \tilde{I}_n^{i}] \tag{97a}$$

$$\tilde{B}_n^{\phi} = 0 \tag{97b}$$

Of course, the elements of the row vectors on the right-hand side of (97a) are given by (96).

The excitation vectors $\tilde{B}_n^{\theta}$ and $\tilde{B}_n^{\phi}$ of (66) are now obtained for the ϕ-polarized wave (91). Replacement of $\underline{W}_{ni}^{p+}$, p = 1,2,3, by $\underline{W}_{ni}^{r+}$, in (39), substitution of (91) and (0, 0) for $(\underline{E}^{i+}, \underline{H}^{i+})$ and $(\underline{E}^{i-}, \underline{H}^{i-})$ in (39), and use of the relationship $\underline{H}^{\phi} = \underline{E}^{\theta}/\eta^+$ yield

$$V_{ni}^{il+} = \langle W_{ni'}^{r+}, \frac{1}{\eta^+} E^{\phi} \rangle \tag{98a}$$

$$V_{ni}^{il-} = 0 \tag{98b}$$

$$V_{ni}^{i} = \langle W_{ni'}^{r+}, \frac{1}{\eta^+} E^{\phi} \rangle \tag{98c}$$

$$I_{ni}^{i} = \langle W_{ni'}^{r+}, \frac{1}{\eta^+} E^{\theta} \rangle \tag{98d}$$

Now, (98) reduces to

$$V^{il+}_{ni} = V^{r\phi}_{ni'} \tag{99a}$$

$$V^{il-}_{ni} = 0 \tag{99b}$$

$$V^{i}_{ni} = V^{r\phi}_{ni'} \tag{99c}$$

$$I^{i}_{ni} = V^{r\theta}_{ni'} \tag{99d}$$

where the V's on the right-hand sides of (99) are given by [12, Eqs. (113), (114), (116), and (117)] with i replaced by i' and k replaced by k^{+}. Since $V^{t\theta}_{ni'}$ and $V^{\phi\phi}_{ni'}$ are even in n and $V^{\phi\theta}_{ni'}$ and $V^{t\phi}_{ni'}$ are odd in n, substitution of (99) into (67) with due regard to (66) gives

$$\tilde{B}^{\theta}_{n} = 0 \tag{100a}$$

$$\tilde{B}^{\phi}_{n} = [\tilde{V}^{il+}_{n} \quad 0 \quad \tilde{V}^{i}_{n} \quad \tilde{I}^{i}_{n}] \tag{100b}$$

where the elements of the row vectors on the right-hand side of (100b) are given by (99). The superscripts θ and ϕ that were first introduced in (64) and (65) had no mnemonic meaning then, but seem to denote the θ and ϕ polarized incident plane waves now in (97) and (100).

To avoid confusion between the right-hand sides of (97a) and (100b) and to achieve harmony with (66), we replace (97a) by

$$\tilde{B}^{\theta}_{n} = [\tilde{V}^{il+\theta}_{n} \quad 0 \quad \tilde{V}^{i\theta}_{n} \quad \tilde{I}^{i\theta}_{n}] \tag{101}$$

and (100b) by

$$\tilde{B}^{\phi}_{n} = [\tilde{V}^{il+\phi}_{n} \quad 0 \quad \tilde{V}^{i\phi}_{n} \quad \tilde{I}^{i\phi}_{n}] \tag{102}$$

According to (96), the ith elements of the row vectors in (101) are given by

$$V^{il+\theta}_{ni} = V^{r\theta}_{ni'}, \quad \underline{W}^{r+}_{ni'} = \underline{W}^{1+}_{ni} \tag{103a}$$

$$V^{i\theta}_{ni} = V^{r\theta}_{ni'}, \quad \underline{W}^{r+}_{ni'} = \underline{W}^{2+}_{ni} \tag{103b}$$

$$I^{i\theta}_{ni} = -V^{r\phi}_{ni'}, \quad \underline{W}^{r+}_{ni'} = \underline{W}^{3+}_{ni} \tag{103c}$$

According to (99), the ith elements of the row vectors in (102) are given by

$$V_{ni}^{il+\phi} = V_{ni'}^{r\phi} \quad , \quad \underline{W}_{ni'}^{r+} = \underline{W}_{ni}^{1+} \tag{104a}$$

$$V_{ni}^{i\phi} = V_{ni'}^{r\phi} \quad , \quad \underline{W}_{ni'}^{r+} = \underline{W}_{ni}^{2+} \tag{104b}$$

$$I_{ni}^{i\phi} = V_{ni'}^{r\theta} \quad , \quad \underline{W}_{ni'}^{r+} = \underline{W}_{ni}^{3+} \tag{104c}$$

The V's on the right-hand sides of (103) and (104) are given by [12, Eqs. (113), (114), (116), and (117)] modified as indicated below (96). The auxiliary equations involving the W's in (103) and (104) determine r and i'. For instance, the values of r and i' in (103a) are such that $\underline{W}_{ni'}^{r+} = \underline{W}_{ni}^{1+}$.

It is now evident that the electric and magnetic currents due to the θ-polarized incident plane wave (90) are given by (73)-(75) and (79)-(81) where the I's and V's in (79)-(81) are the elements (68a) of $\tilde{X}_n^{\theta}$ obtained by solving (65a) for non-negative values of n with $\tilde{B}_n^{\theta}$ given by (101). Similarly, the currents due to the ϕ-polarized wave (91) are given by (76)-(78) and (82)-(84) where the I's and V's in (82)-(84) are the elements (68b) of $\tilde{X}_n^{\phi}$ obtained by solving (65b) with $\tilde{B}_n^{\phi}$ given by (102). Because the testing functions $\underline{W}_{ni}^{r+}$, and normalized fields $\underline{E}^{\theta}/\eta^{+}$ and $\underline{E}^{\phi}/\eta^{+}$ all have the dimension of (1/distance), the elements of the excitation vectors $\tilde{B}_n^{\theta}$ of (101) and $\tilde{B}_n^{\phi}$ of (102) are dimensionless. Since the elements of the moment matrix T_n are dimensionless, the elements of $\tilde{X}_n^{\theta}$ and $\tilde{X}_n^{\phi}$ obtained by solving (65) are also dimensionless. As a result, the Fourier coefficients (79)-(84) of the currents are dimensionless. This is not surprising because, due to the facts that an electric current has the same dimension as its magnetic field and that a magnetic current has the same dimension as its electric field, the electric currents (73)-(74) and (76)-(77) must have the same dimension as (90c) and (91c) and the magnetic currents (75) and (78) must have the same dimension as (90b) and (91b).

VI. NUMERICAL RESULTS

A computer program was written to calculate the Fourier coefficients (87)-(89) of the electric and magnetic currents due to the θ-polarized wave (90), which is generally obliquely incident. This program will be described and listed along with sample input and output data in a forthcoming report. The ϕ-polarized wave (91) was avoided for fear of making the program unwieldy. According to the exposition in Sections IV and V, the Fourier coefficients of the currents due to the ϕ-polarized wave can easily be obtained by making two minor changes in the computational procedure for the θ-polarized wave. These changes are replacement of (101) by (102) and interchange of the factors ε_n and $2j$ in (79)-(81) and (87)-(89).

In this section, the magnitudes of the Fourier coefficients (87)-(89) of the electric and magnetic currents due to an axially incident plane wave traveling in the minus z direction are plotted for four different objects of revolution. Specifically, the incident wave is given by (90) with $\theta_t = 0$. At $\theta_t = 0$, the excitation vector (101), being obtained from [12, Eqs. (113), (114), (116), and (117)], is zero for $n \neq \pm 1$. Hence, the only non-zero Fourier coefficients in (87)-(89) are those for which n=1. These Fourier coefficients were calculated by using the computer program introduced in the previous paragraph. It is evident from (73)-(75) and (90) that expressions (87) and (88) are ratios of the electric currents to the incident magnetic field and that expressions (89) are ratios of the magnetic currents to the incident electric field.

In Figs. 7-9, the magnitudes of the Fourier coefficients (87)-(89) of the currents on the object of Fig. 6 are plotted by means of symbols. The key for the symbols is given by

$\square$ $|J_1^{t+0}(\bar{t}_j')|$ on conducting surfaces (105a)

$\bigcirc$ $|J_1^{\phi+0}(t_j')|$ on conducting surfaces (105b)

$\wedge$ $|J_1^{t+0}(\bar{t}_j^+)|$ in the aperture (105c)

$+$ $|J_1^{\phi+0}(t_j^+)|$ in the aperture (105d)

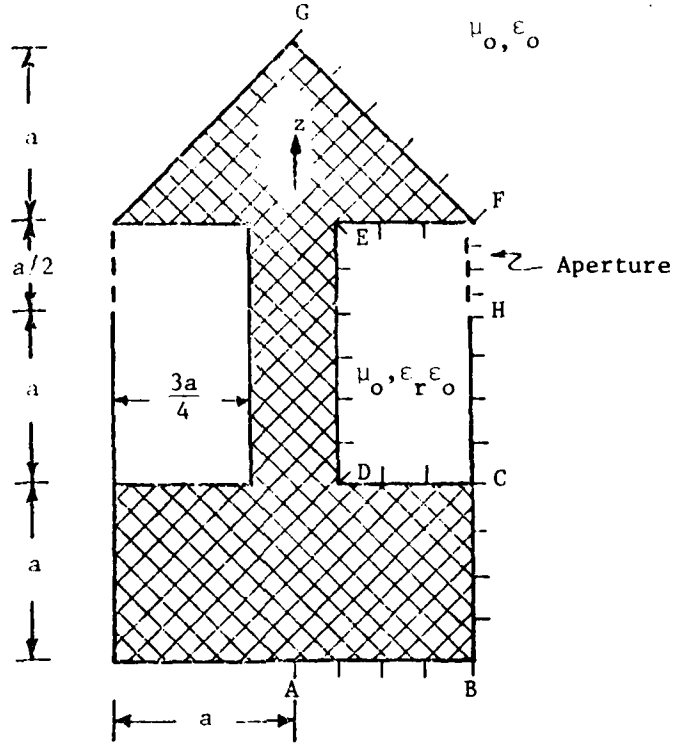

Fig. 6. Perfectly conducting arrow with thick washer dielectric region.

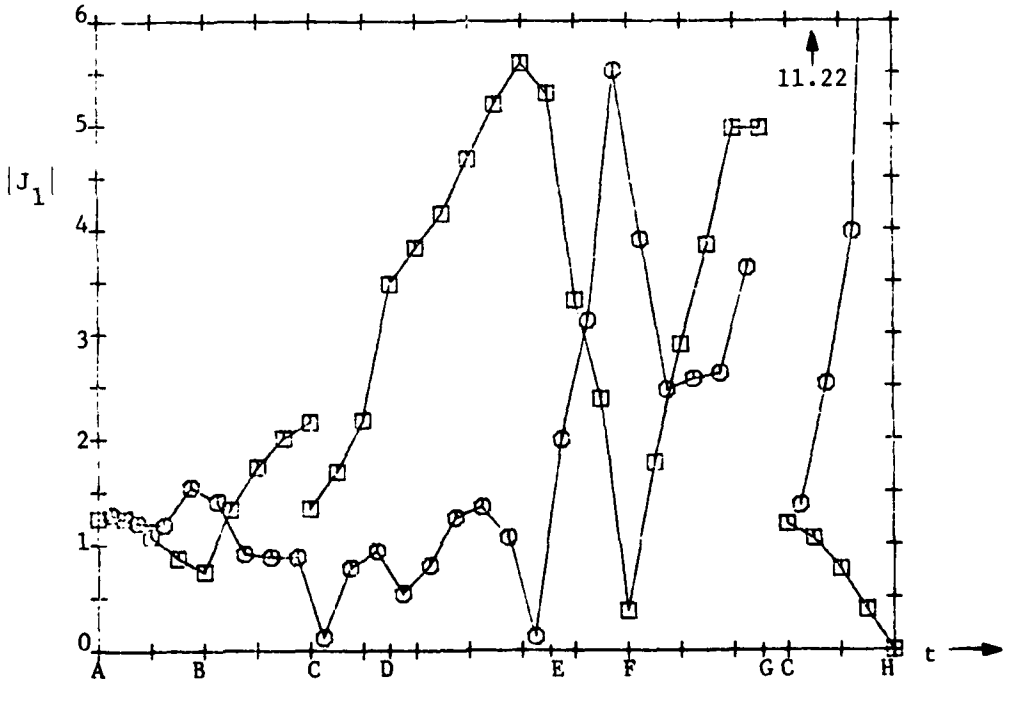

Fig. 7. E-field solution for electric current on conducting surfaces of Fig. 6. $a = 0.2\lambda$, $\varepsilon_r = 1$.

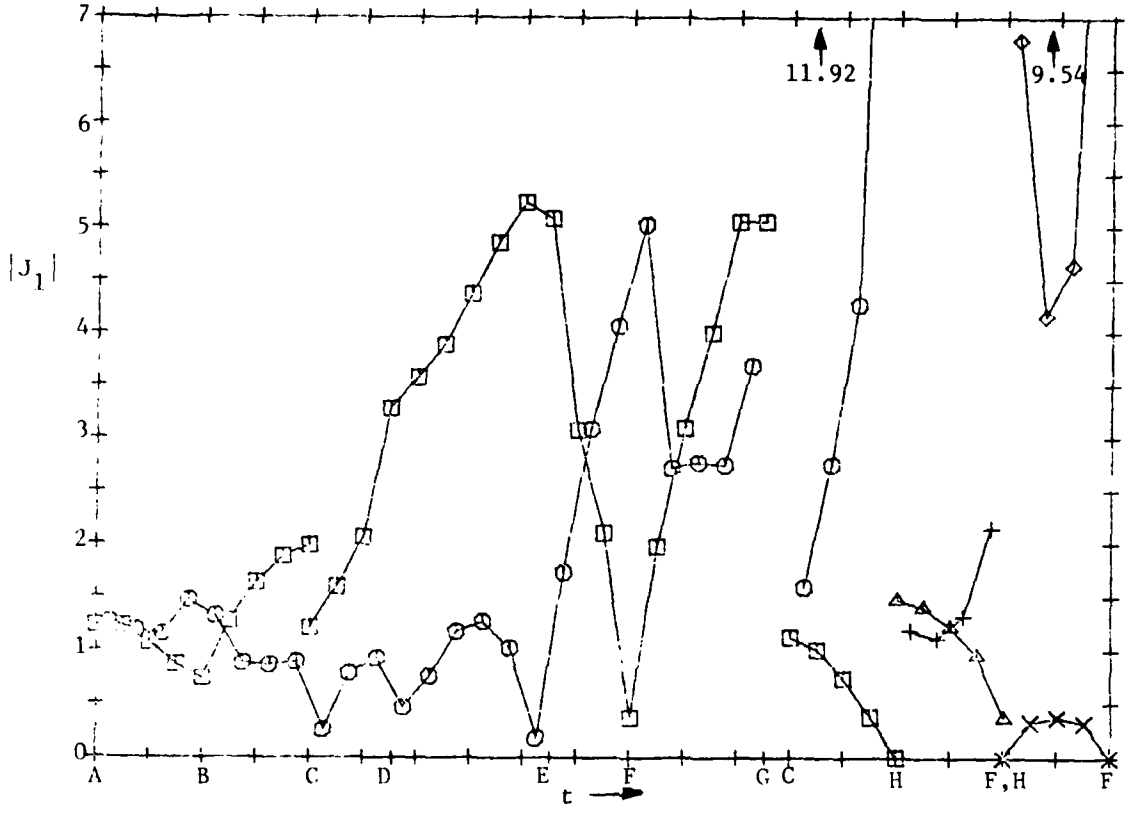

Fig. 8. Currents on object of Fig. 6. Aperture formulation, a=0.2λ, ε_r=1.

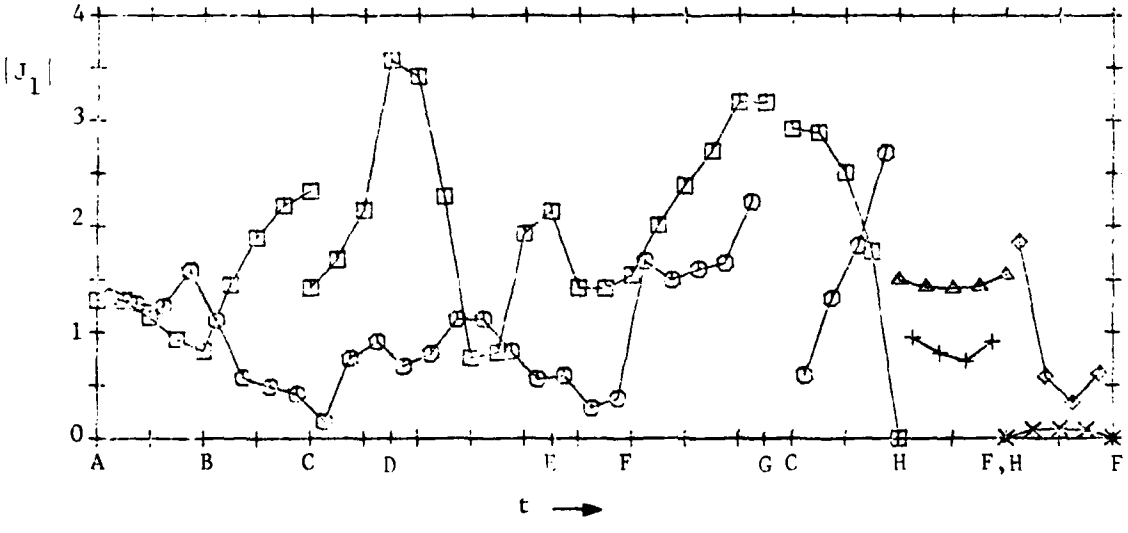

Fig. 9. Currents on object of Fig. 6. Aperture formulation, a=0.2λ, ε_r=4.

$\times$ $|M_1^{t\theta}(\bar{t}_j^{+})|$ in the aperture (105e)

$\diamond$ $|M_1^{\phi\theta}(t_j^{+})|$ in the aperture (105f)

In (105a) and (105b), the plus sign applies on S^+ and the minus sign applies on S^-. The surfaces S^+ and S^- merge on the infinitely thin conducting flange from C to H in Fig. 6. There, (105a) and (105b) are replaced by

$|J_1^{t+\theta}(\bar{t}_j^{+}) - J_1^{t-\theta}(\bar{\bar{t}}_\ell^{-})|$ on the thin flange (106a)

$|J_1^{\phi+\theta}(t_j^{+}) - J_1^{\phi-\theta}(t_m^{-})|$ on the thin flange (106b)

where ℓ is such that both $\bar{t}_j^{+}$ and $\bar{\bar{t}}_\ell^{-}$ are located at the same point on the flange and m is such that both t_j^{+} and t_m^{-} are located at the same point on the flange. The expressions whose magnitudes are being taken in (106) are the Fourier coefficients of the electric current induced on the flange. In general, the electric current induced on an infinitely thin perfectly conducting surface is the sum of the exterior and interior currents. However, because $-\underline{J}^-$ is used in Fig. 3, the electric current induced on the flange in Fig. 6 is $\underline{J}^+ - \underline{J}^-$. Thus, the difference rather than the sum of coefficients is required in (106). All of expressions (105) and (106) are plotted in each of Figs. 8 and 9. However, only the expressions on the conducting surfaces, namely (105a), (105b), (106a), and (106b) are plotted in Fig. 7. Actually, the expressions plotted in Fig. 7 are not (105a), (105b), (106a), and (106b) themselves but expressions comparable to them.

For simplicity, the vertical axes in Figs. 7-9 are labeled $|J_1|$. The horizontal axes are labeled t rather than t^+ or t^-. Here, t represents arc length between the points A,B,C,... designated in Fig. 6. The t components of (the Fourier coefficients of) the currents, namely (105a), (105c), (105e), and (106a), are plotted at the tick marks in Fig. 6. These tick marks represent the data points (11). The ϕ components of the currents, namely (105b), (105d), (105f), and (106b), are plotted at points midway between the tick marks in Fig. 6. In Figs. 7-9, the symbols used to

plot (105) and (106) are connected by straight line segments to improve readability. To avoid congestion, the aperture region from H to F in Fig. 6 is depicted twice in each of Figs. 8 and 9, once for plotting the electric currents (105c) and (105d) and once for plotting the magnetic currents (105e) and (105f). The following argument reveals that the t axes in Figs. 7-9 are not always drawn to scale. Not all data points in Fig. 6 are equally spaced. For instance, the data points from F to G are not quite as dense as those from A to B. More obviously, the data points in the aperture are twice as dense as those from A to B. However, all data points are equally spaced along the t axes in Figs. 7-9. Incidentally, the proper density of data points, or rather triangle functions, in the aperture is discussed in [8].

The currents in Fig. 7 were obtained by means of the E-field solution, the currents in Figs. 8 and 9 by means of the aperture formulation, and, if the reader will please glimpse forward, the currents in Fig. 15 by means of the H-field solution. The E-field solution is that of [12] with

$$\left.\begin{aligned} n_t &= 2 \\ n_\phi &= 20 \\ n_T &= 2 \end{aligned}\right\} \tag{107}$$

where n_t, n_ϕ, and n_T appear in the Gaussian quadrature formulas [12, Eqs. (62), (64), and (132)], respectively. The H-field solution is that of [14] with the values of n_t, n_ϕ, and n_T therein given by (107). Specifically, n_t, n_ϕ, and n_T appear in [14, Eqs. (35), (36), and (79)]. The roles played by n_t, n_ϕ, and n_T in [14] are similar to the roles played by n_t, n_ϕ, and n_T in [12]. The aperture formulation refers to the solution (87)-(89) developed in the present report. In view of (68a), the I's and V's in (87)-(89) are given by the solution $\vec{X}_1^0$ to (65a). In Section IV, the elements of the moment matrix T_1 were expressed in terms of the elements of matrices similar to the moment matrices used in [12] and [14]. In Section V, the elements of $\vec{B}_1^0$ in (65a) were expressed in terms of the elements of the plane wave excitation vectors used in [12]. The currents

attributed to the aperture formulation were obtained by calculating T_1 and $B_1^{+\theta}$ with n_t, n_ϕ, and n_T given by (107).

The E-field solution for the electric current induced on the conducting surfaces of the object in Fig. 6 was constructed by using two generating curves. The first one is ABCDEFG and the second one extends from the tick mark directly below C to the point H. Since the computer program in [12] is designed to handle only one generating curve, the two (short) curves were connected to form one long curve, and then all matrix elements associated with the line connecting the two short curves were deleted. The matrix elements associated with the first pulse function on the second short curve were also deleted because that pulse function is a duplicate of one of the pulse functions on the first short curve. With this arrangement, two independent triangle functions are centered at C. Because each of these triangle functions satisfies Kirchhoff's current law at C, the resulting E-field solution for the t component of the induced electric current satisfies Kirchhoff's current law at C. The t component of the induced electric current obtained by means of the aperture formulation also satisfies Kirchhoff's current law at C. However, satisfaction of Kirchhoff's current law by the t component of the induced electric current at C is masked in Figs. 7-9 because magnitudes of currents rather than real and imaginary parts of currents are plotted there.

The t component of the induced electric current is zero at H in Fig. 7 because no triangle function is centered there. The t component (106a) of the induced electric current is zero at H in Figs. 8 and 9 because the two J's in (106a) are equal to each other at H. These two J's have to be equal to each other at H because they are both equal to the aperture current there.

It is obvious that the E-field solution for the t component of the induced electric current has to be continuous at F in Fig. 6. The following reasoning shows that the t component of the induced electric current obtained by using the aperture formulation is also continuous at F. Because the t direction is the same as the t^+ direction on the G side of F, the t component of the induced electric current is $J_1^{t+\theta}(t^+)$ there. Now,

t and t^- are oppositely directed on the E side of F and there is a compensating minus sign on $\underline{J}^-$ in Fig. 3 so that the t component of the induced electric current is $J_1^{t-\theta}(t^-)$ on the E side of F. However, $J_1^{t+\theta}(t^+) = J_1^{t-\theta}(t^-)$ at F because they are both equal to the aperture current there. Hence, the t component of the induced electric current obtained by using the aperture formulation is continuous at F.

The notation previously developed with specific reference to Figs. 6-9 and 15 applies not only to these figures but also to Figs. 10-14 and 16-22. The object in Fig. 10 differs from the exemplary object in Fig. 1 in that neither the exterior surface S^+ nor the interior surface S^- has a part above the aperture in Fig. 10. Nevertheless, the computer program mentioned in the first paragraph of this section is still applicable. Figure 11 shows currents on the spherical shell and associated aperture region of Fig. 10 when $\varepsilon_r = 1$. The currents plotted from A to B in Fig. 11 are the electric currents (106) induced on the conducting shell.

The following reasoning shows that the E-field solution for the electric current induced on the conducting shell in Fig. 10 is exactly the same as the solution obtained by means of the aperture formulation when $\varepsilon_r = 1$. When partitioned, (31) consists of four matrix equations. The first two of these equations are

$$Z_n^{11+}\,\vec{I}_n^{1+} + Z_n^{12+}\,\vec{I}_n - Y_n^{13+}\,\vec{V}_n = \vec{V}_n^{i1+} \tag{108a}$$

$$\eta_r Z_n^{11-}\,\vec{I}_n^{1-} + \eta_r Z_n^{12-}\,\vec{I}_n - Y_n^{13-}\,\vec{V}_n = \vec{V}_n^{i1-} \tag{108b}$$

Since the conducting surface in Fig. 10 is infinitely thin, the surfaces S^+ and S^- exemplified in Fig. 1 are identical. Furthermore, $\varepsilon_r = 1$ and $\eta_r = 1$ so that the superscripts + and - attached to the Z's and Y's in (108) lose their distinction. Hence, the difference between (108a) and (108b) reduces to

$$Z_n^{11+}[\vec{I}_n^{1+} - \vec{I}_n^{1-}] = \vec{V}_n^{i1+} - \vec{V}_n^{i1-} \tag{109}$$

Because the elements of $[\vec{I}_n^{1+} - \vec{I}_n^{1-}]$ can be interpreted as the unknown

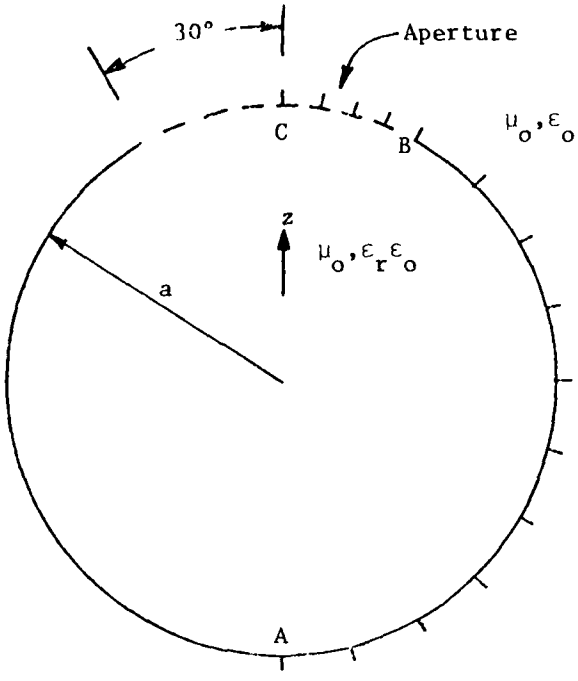

Fig. 10. Infinitely thin perfectly conducting spherical shell with aperture and interior dielectric region

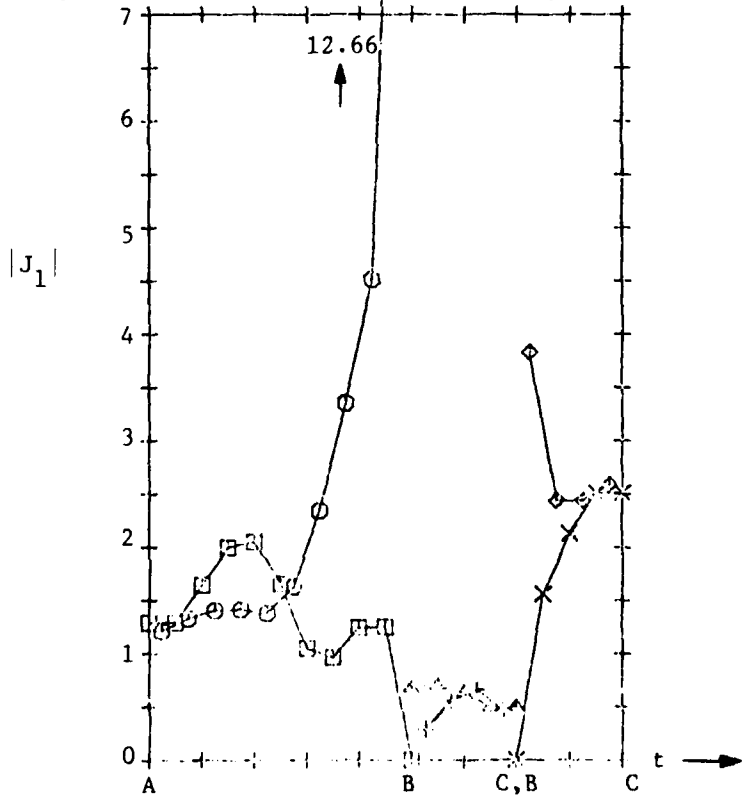

Fig. 11. Currents on object of Fig. 10. Aperture formulation, $k^+a = 2.5$, $\varepsilon_r = 1$.

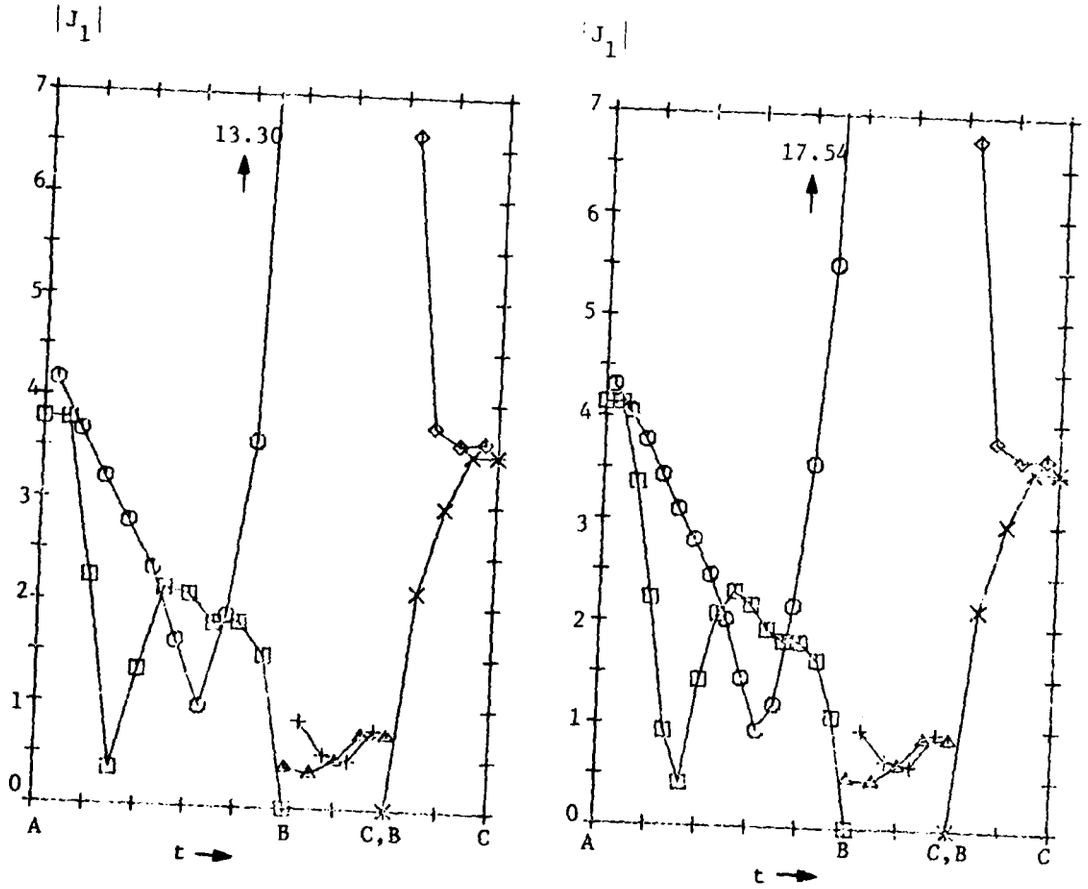

Fig. 12. Currents on object of Fig. 10. Aperture formulation, $k^+a = 2.5$, $\epsilon_r = 2$. (a) 10 intervals from A to B as in Fig. 10. (b) 15 intervals from A to B.

coefficients appearing in the expansion of the electric current induced on the shell, (109) is precisely the matrix equation for the E-field solution. As a result, the E-field solution for the electric current induced on the shell in Fig. 10 is exactly the same as the electric current plotted from A to B in Fig. 11.

The magnetic currents (105e) and (105f) plotted from B to C in Fig. 11 are comparable, respectively, to the functions $|g(\theta)|$ and $|f(\theta)|$ appearing in [15, Fig. 7]. The horizontal axes in [15, Fig. 7] and Fig. 11 run in opposite directions. The statement that ka = 2.75 in the caption of [15, Fig. 7] is incorrect because ka is really 2.5 there. The currents shown in Fig. 12a were calculated by using the data points designated in Fig. 10. However, the currents shown in Fig. 12b were calculated with the curve from A to B in Fig. 10 divided into not 10 but 15 equal intervals. For Fig. 12b, the data points in the aperture were those designated in Fig. 10.

The object in Fig. 13 was obtained by taking a perfectly conducting solid sphere of radius a centered at the origin and replacing the conducting material in the region $|z| < a \sin 15°$ by dielectric material characterized by $(\varepsilon_o, \varepsilon_r\varepsilon_o)$. The E-field and H-field solutions for the electric current induced on the conducting surfaces of Fig. 13 are shown in Figs. 14 and 15, respectively. These solutions were obtained by connecting the generating curves ABC and DEF in Fig. 13 to obtain the single curve ABCDEF and then deleting the matrix elements associated with the connecting line CD. Divisions by zero were avoided by arbitrarily setting $k^+\rho$ equal to 1 midway between C and D. Here, ρ is the distance from the z axis.

The currents shown in Figs. 16 and 17 are on the object of Fig. 13 and were obtained from the aperture formulation. The object in Fig. 13 differs from the exemplary object in Fig. 1 in that the parts of S^- above and below the aperture are disjoint in Fig. 13. However, the computer program mentioned in the first paragraph of this section allows for this. The induced electric currents from A to C and from D to F are slightly different from each other in Figs. 14-16. The induced electric current on the conducting surfaces of Fig. 13 obtained from the aperture formulation when $\varepsilon_r = 1$ differs from the E-field solution for the induced

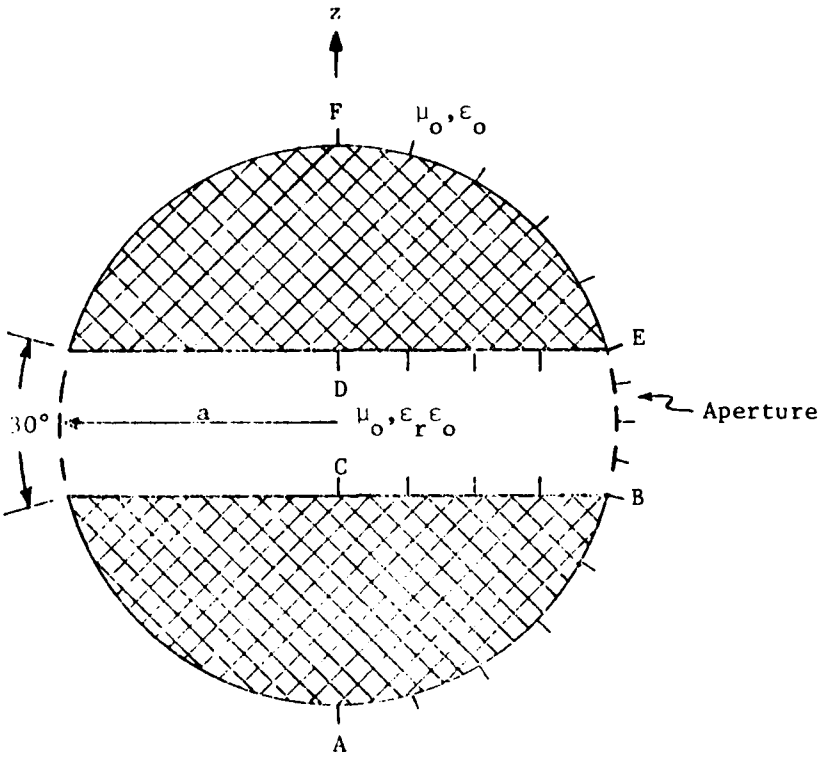

Fig. 13. Two perfectly conducting portions of a sphere separated by a dielectric region.

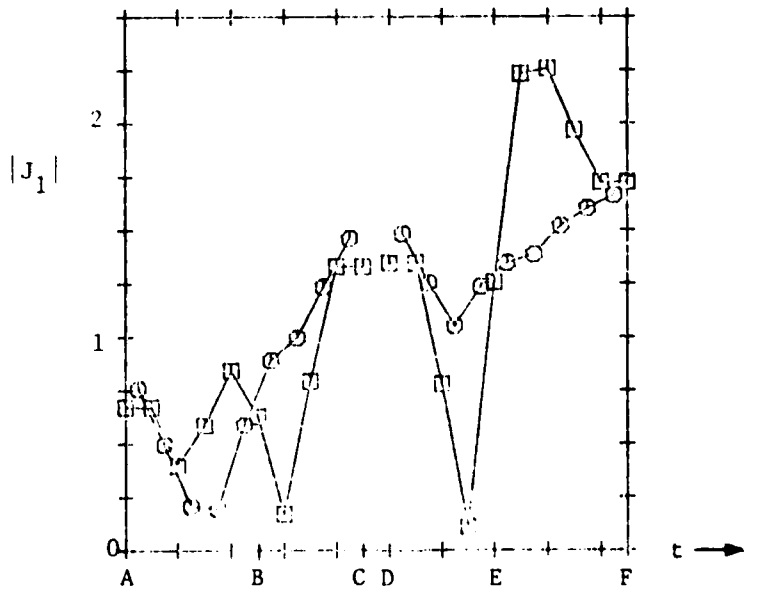

Fig. 14. E-field solution for electric current on conducting surfaces of Fig. 13. $k^+a = 2.5$, $\varepsilon_r = 1$.

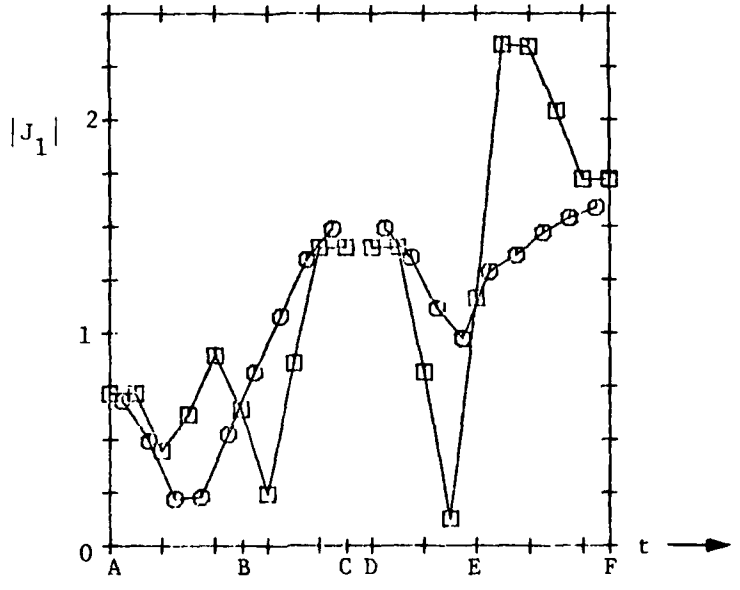

Fig. 15. H-field solution for electric current on conducting surfaces of Fig. 13. $k^+a = 2.5$, $\varepsilon_r = 1$.

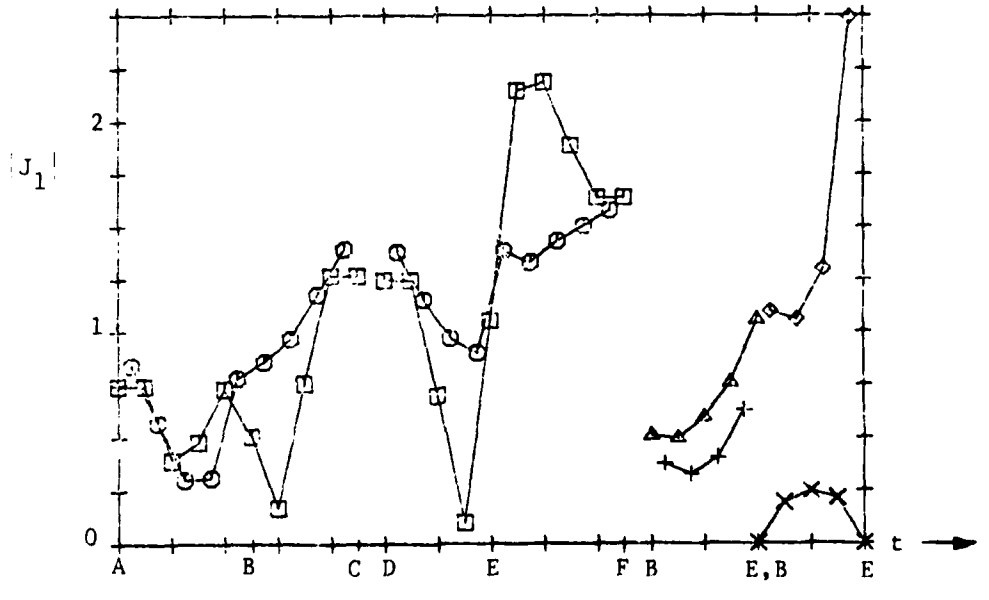

Fig. 16. Currents on object of Fig. 13. Aperture formulation, $k^+a = 2.5$, $\varepsilon_r = 1$.

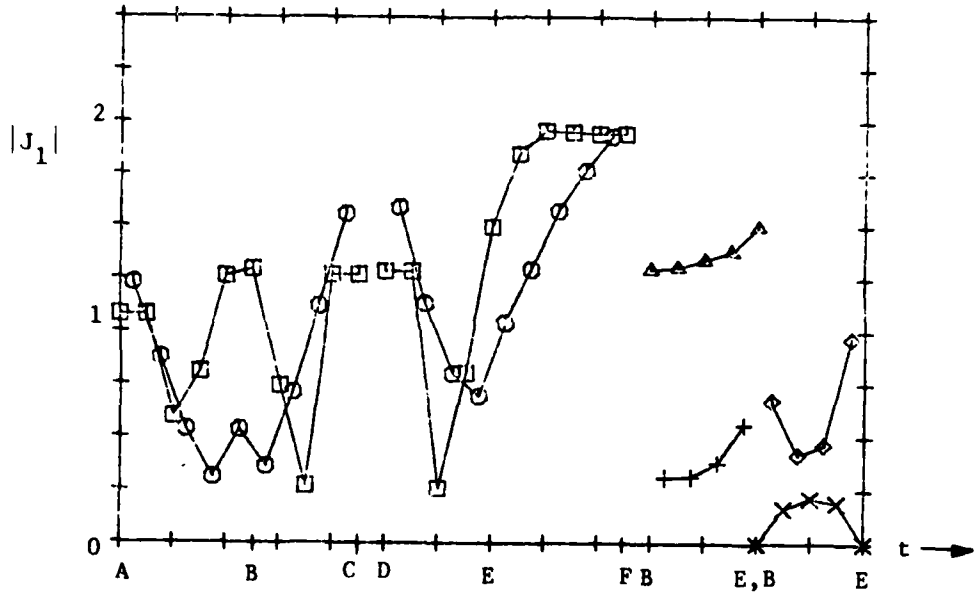

Fig. 17. Currents on object of Fig. 13. Aperture formulation, $k^{+}a = 2.5$, $\varepsilon_r = 2$.

electric current because of the following reasoning. Of the triangle functions used in the aperture formulation, those centered at B and E are essential to the induced electric current. However, these triangle functions extend into the aperture. On the other hand, all of the triangle functions used in the E-field solution are confined to the conducting surfaces. In this respect, the aperture formulation differs from the E-field solution.

Figures 19-22 show currents on the object of Fig. 18. On the object of Fig. 18, EFB is the generating curve of the aperture. The object in Fig. 18 differs from the exemplary object in Fig. 1 in that neither the external surface S^+ nor the internal surface S^- has a part below the aperture in Fig. 18. However, the computer program mentioned in the first paragraph of this section allows for this. As seen from Figs. 19-21, the E-field solution, the H-field solution, and the aperture formulation each give slightly different results for the electric current induced on ABCD in Fig. 18. The E-field solution and the aperture formulation give different results for this current because in the aperture formulation the conductor is coupled to the aperture at point B in Fig. 18.

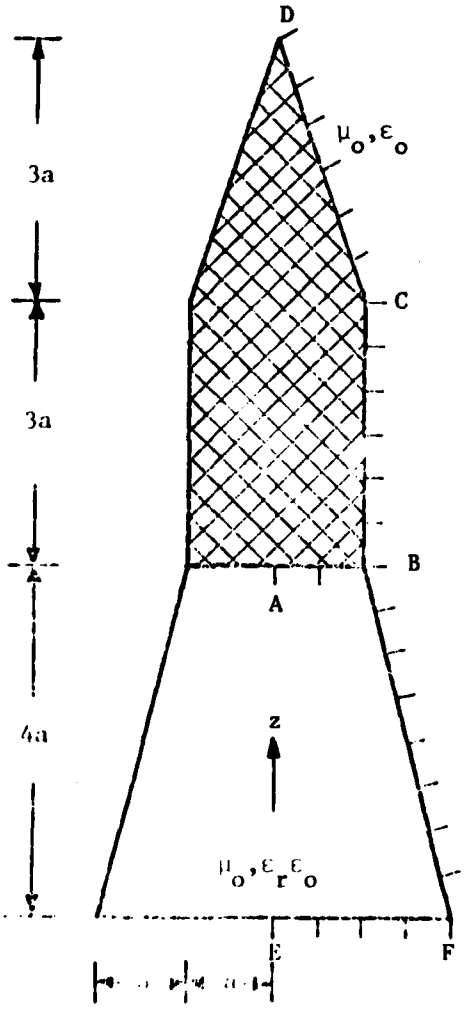

Fig. 18. Perfectly conducting closed silo with dielectric base.

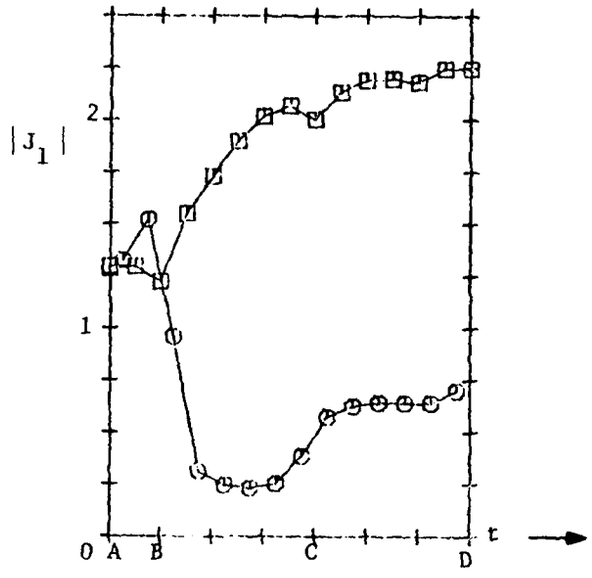

Fig. 19. E-field solution for electric current on conducting surface of Fig. 18. $a = 0.1\lambda$, $\varepsilon_r = 1$.

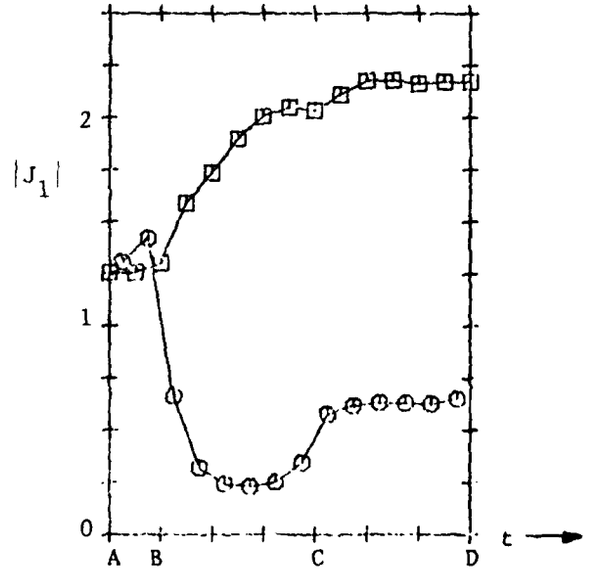

Fig. 20. H-field solution for electric current on conducting surface of Fig. 18. $a = 0.1\lambda$, $\varepsilon_r = 1$.

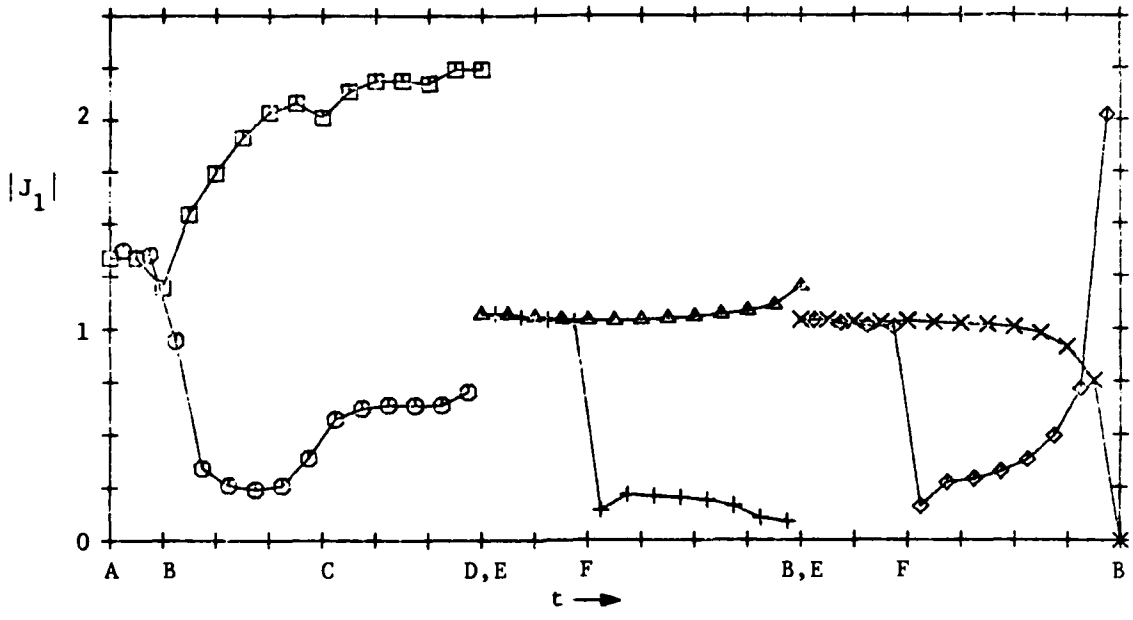

Fig. 21. Currents on object of Fig. 18. Aperture formulation, $a = 0.1\lambda$, $\varepsilon_r = 1$.

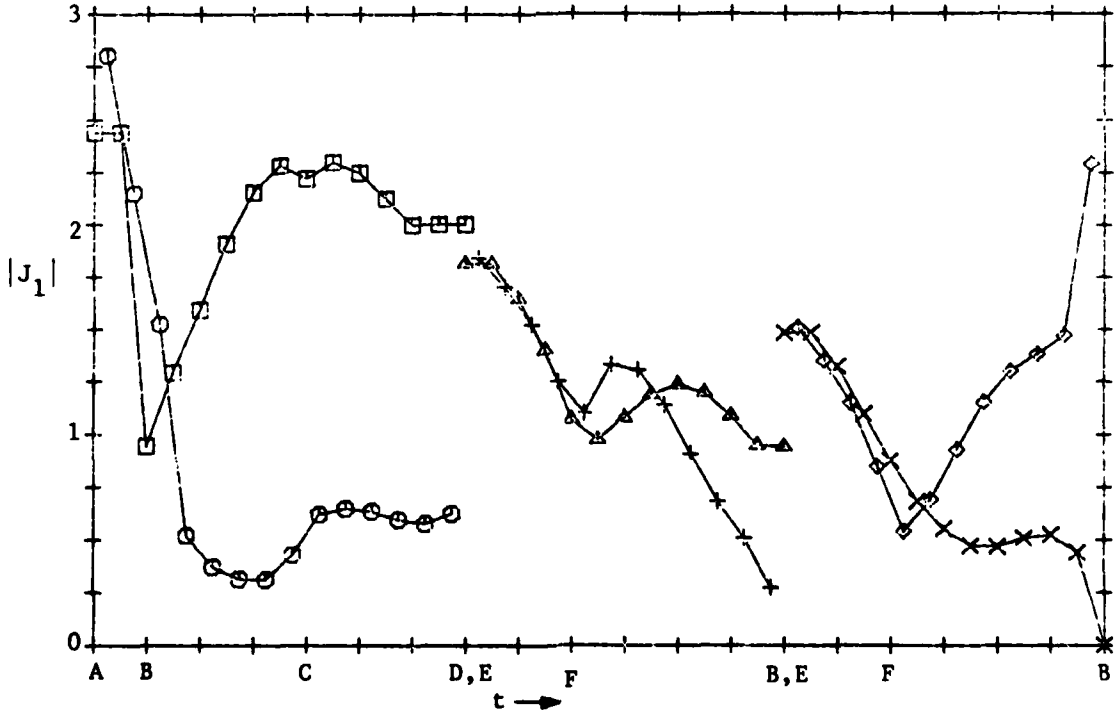

Fig. 22. Currents on object of Fig. 18. Aperture formulation, $a = 0.1\lambda$, $\varepsilon_r = 4$.

REFERENCES

[1] J. R. Mautz and R. F. Harrington, "Electromagnetic Scattering from a Homogeneous Material Body of Revolution," AEÜ, vol. 33, No. 2, pp. 71-80, February, 1979.

[2] A. W. Glisson and D. R. Wilton, "Simple and Efficient Numerical Methods for Problems of Electromagnetic Radiation and Scattering from Surfaces," IEEE Trans. Antennas Propagat., vol. AP-28, No. 5, pp. 593-603, September 1980.

[3] T. K. Wu and L. L. Tsai, "Scattering from Arbitrarily-shaped Lossy Dielectric Bodies of Revolution," Radio Sci., vol. 12, pp. 709-718, Sept.-Oct. 1977.

[4] R. J. Pogorzelski, "On the Numerical Computation of Scattering from Inhomogeneous Penetrable Objects," IEEE Trans. Antennas Propagat., vol. AP-26, No. 4, pp. 616-618, July 1978.

[5] L. N. Medgyesi-Mitschang and C. Eftimiu, "Scattering from Axisymmetric Obstacles Embedded in Axisymmetric Dielectrics: The Method of Moments Solution," Appl. Phys., vol. 19, pp. 275-285, 1979.

[6] H. K. Schuman, "Improved Bodies of Revolution," Report RADC-TR-80-389, Rome Air Development Center, Griffiss Air Force Base, New York, November 1980, A096048.

[7] R. F. Harrington, Time-Harmonic Electromagnetic Fields, McGraw-Hill Book Co., New York, 1961.

[8] H. K. Schuman and D. E. Warren, "Aperture Coupling in Bodies of Revolution," IEEE Trans. Antennas Propagat., vol. AP-26, No. 6, pp.778-783, November 1978.

[9] R. F. Harrington and J. R. Mautz, "An Impedance Sheet Approximation for Thin Dielectric Shells," IEEE Trans. Antennas Propagat., vol. AP-23, pp. 531-534, July, 1975.

[10] J. R. Mautz and R. F. Harrington, "Boundary Formulations for Aperture Coupling Problems," AEÜ, vol. 34, No. 9, pp. 377-384, September 1980.

[11] R. F. Harrington, Field Computation by Moment Methods, The Macmillan Co., New York, 1968.

[12] J. R. Mautz and R. F. Harrington, "An Improved E-field Solution for a Conducting Body of Revolution," Report RADC-TR-80-194, Rome Air Development Center, Griffiss Air Force Base, New York, June 1980.

[13] J. R. Mautz and R. F. Harrington, "H-field, E-field, and Combined Field Solutions for Bodies of Revolution," Report RADC-TR-77-109, N.T.I.S. No. ADA 040379, Rome Air Development Center, Griffiss Air Force Base, New York, June 1977, A040379.

[14] J. R. Mautz and R. F. Harrington, "An H-field Solution for a Conducting Body of Revolution," Report RADC-TR-80-362, Rome Air Development Center, Griffiss Air Force Base, New York, November 1980, A096313.

[15] T.B.A. Senior and G. A. Desjardins, "Electromagnetic Field Penetration into a Spherical Cavity," IEEE Trans. Electromagn. Compat., vol. EMC-16, No. 4, pp. 205-208, November 1974.

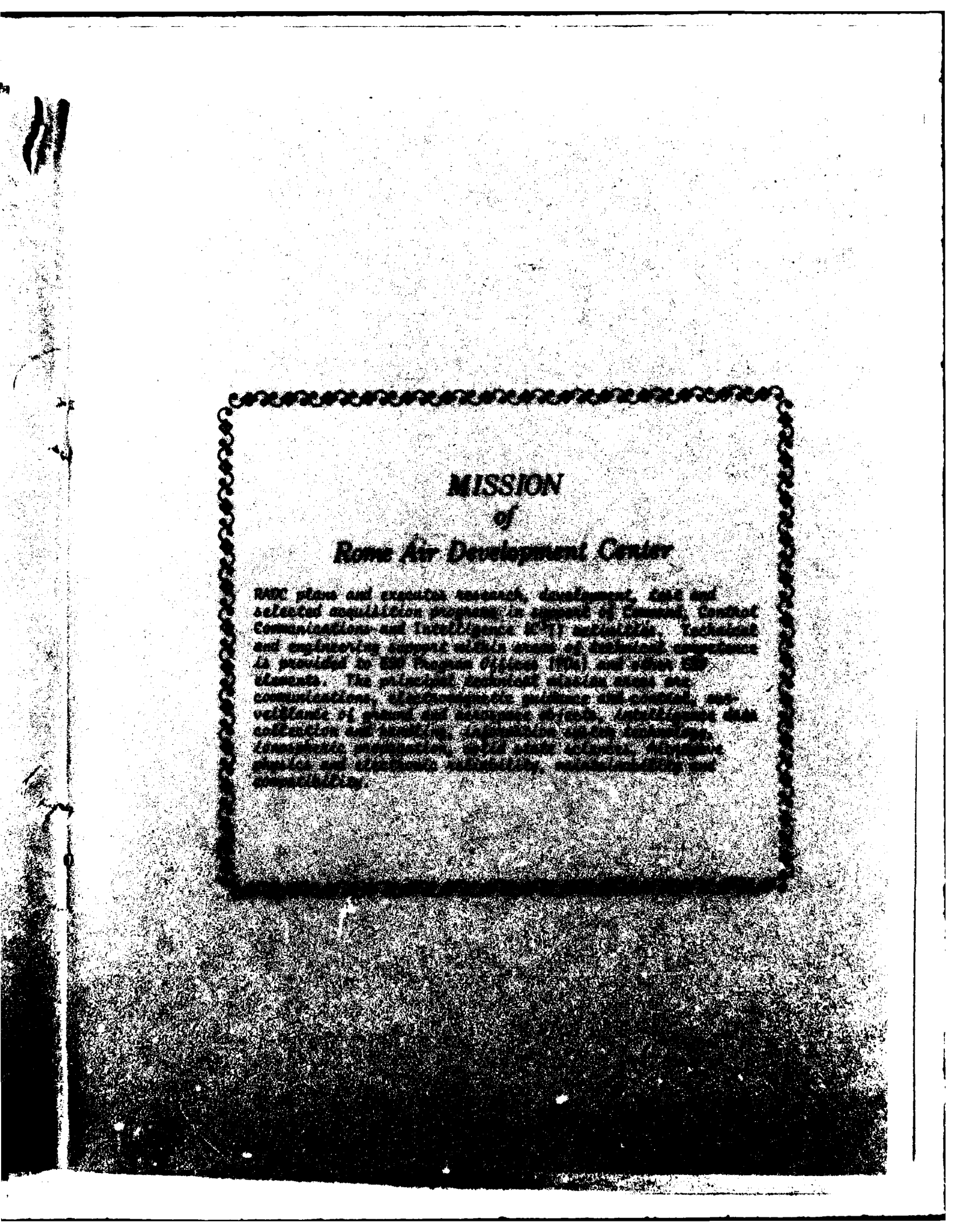
MISSION
of
Rome Air Development Center

END

DATE
FILMED

1-82

DTIC